nature communications

Article

https://doi.org/10.1038/s41467-025-60286-3

ACE2 from *Pipistrellus abramus* bats is a receptor for HKU5 coronaviruses

Received: 17 December 2024

Accepted: 20 May 2025

Published online: 28 May 2025

Check for updates

Nicholas J. Catanzaro[1,5], Ziyan Wu[2,5], Chengcheng Fan[2], Victoria Jefferson[3], Anfal Abdelgadir[1], Alexandra Schäfer[1], Boyd L. Yount[1], Pamela J. Bjorkman[2], Ralph Baric[1,4] & Michael Letko[3]

The merbecovirus subgenus of coronaviruses includes Middle East Respiratory Syndrome Coronavirus (MERS-CoV), a zoonotic pathogen transmitted from dromedary camels to humans that causes severe respiratory disease. Viral discovery efforts uncover hundreds of merbecoviruses in different species across multiple continents, but few are studied under laboratory conditions, leaving basic questions regarding their human threat potential unresolved. Viral entry into host cells is a critical step for transmission between hosts. Here, we develop and apply a scalable approach to assesses novel merbecovirus cell entry across the entire merbecovirus subgenus. Merbecoviruses are sorted into clades based on the receptor-binding domain of the spike glycoprotein. Receptor tropism is clade-specific, with the clade including MERS-CoV using DPP4 and multiple clades using ACE2, including HKU5 bat coronaviruses. Mutational analysis identifies possible structural limitations to HKU5 adaptability and a cryo-EM structure of the HKU5-20s spike trimer reveals only 'down' RBDs.

Middle East Respiratory Syndrome Coronavirus (MERS-CoV) was first discovered in the middle east in 2012 as a cause of severe respiratory illness in humans with high mortality[1]. Field studies have shown that MERS-CoV is endemic in dromedary camels in the region and routinely transmits to humans, sustaining a slow but continual regional outbreak[2,3]. MERS-CoV is the prototypic member of the merbecovirus subgenus of beta-coronaviruses. Virus discovery efforts have uncovered hundreds of merbecoviruses circulating among diverse wildlife across multiple continents[4–13]. As is true with most of the global virome, the majority of all sequenced coronaviruses have never been isolated or molecularly characterized and therefore their threat of spillover into humans remains unknown.

Coronaviruses must enter the cells and replicate to enable efficient transmission between species. MERS-CoV cell entry is mediated by the viral spike protein through several viral-host interactions: (1) the N-terminal domain of spike attaches virus to lectins present on the host cell surface, (2) the receptor binding domain (RBD) binds to the host cell receptor molecule, (3) and receptor binding reorganizes structural elements in the S2 subunit of the spike protein that mediate membrane fusion and subsequent cell entry[14–16]. Each function is performed by a separate region of the spike protein, the RBD being responsible for the core interaction with the host receptor[17–20]. While MERS-CoV uses dipeptidyl peptidase IV (DPP4) as its host receptor to infect cells, several studies have shown that some bat merbecoviruses do not use DPP4 and instead use angiotensin-converting enzyme 2 (ACE2) to infect their hosts[12,21–24].

Similar to other beta-coronaviruses, the RBD in merbecovirus spike proteins is a single, contiguous domain located in the N-terminal half of the spike sequence, and it folds as a structurally stable unit that engages with the host receptor (Fig. 1a, b). To reduce cost of viral gene synthesis while maintaining the ability to study viral protein function, we previously employed a method to replace the RBD of a

[1]Department of Microbiology and Immunology, University of North Carolina at Chapel Hill, Chapel Hill, NC, USA. [2]Division of Biology and Biological Engineering, California Institute of Technology, Pasadena, CA, USA. [3]Paul G. Allen School for Global Health, Washington State University, Pullman, WA, USA. [4]Department of Epidemiology, Gillings School of Global Public Heath, University of North Carolina at Chapel Hill, Chapel Hill, NC, USA. [5]These authors contributed equally: Nicholas J. Catanzaro, Ziyan Wu. e-mail: michael.letko@wsu.edu

https://doi.org/10.1038/s41467-025-60286-3

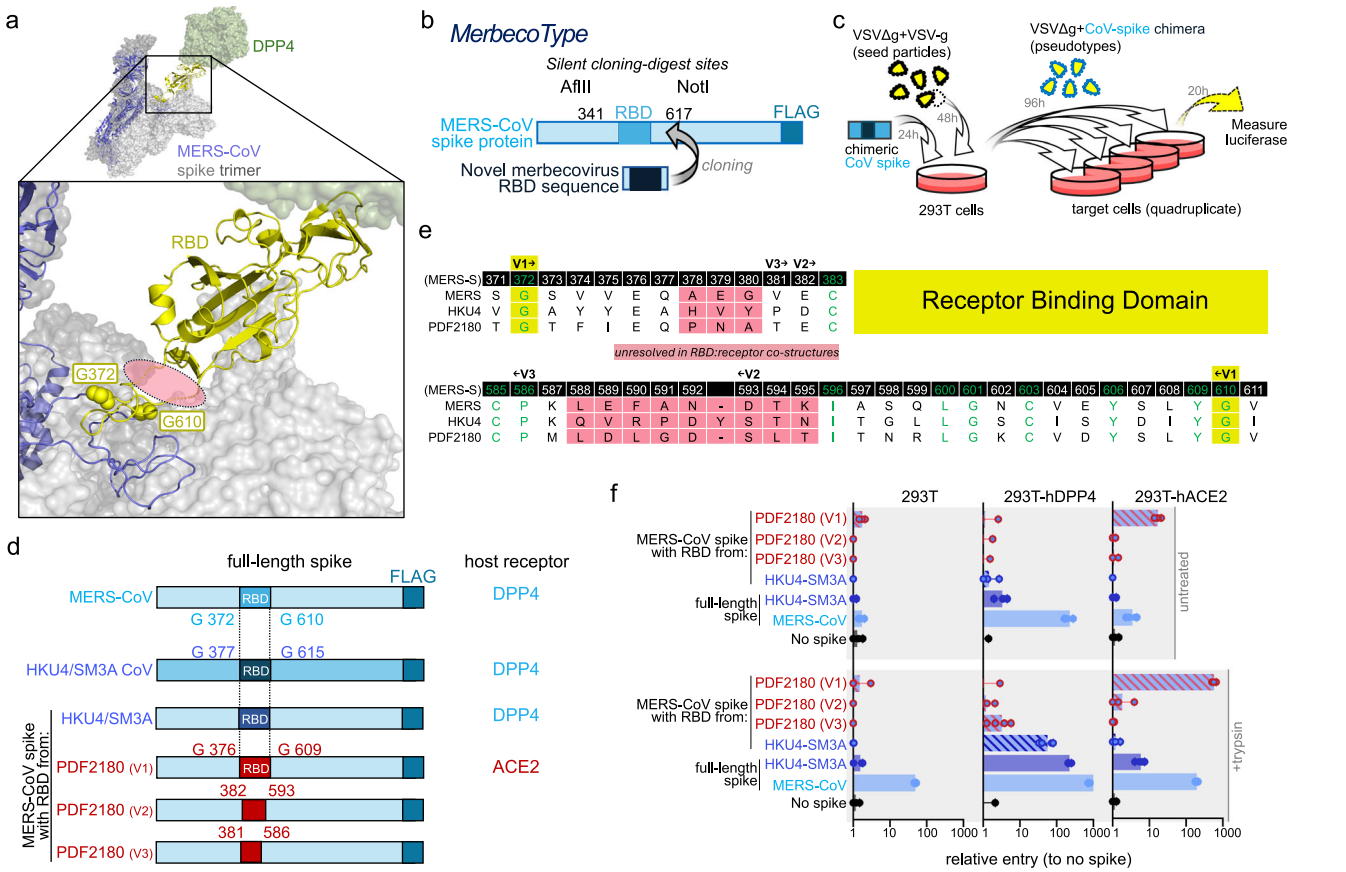

Fig. 1 | Identification of the functional RBD in merbecoviruses. a The receptor binding domain in merbecoviruses engages the host receptor, DPP4 (PDB ID: 4L72, 5×59). Conserved glycines marking the functional RBD boundaries are indicated in yellow spheres. **b** Overview of MERS-CoV spike design for RBD replacement. **c** Chimeric spikes are used to generate single-cycle pseudotyped VSV reporter particles. **d** Overview of chimeric spike designs. **e** Amino acid sequence alignment of region flanking the RBD in merbecoviruses. **f** 293 T cell lines expressing indicated receptors were infected with pseudotypes and luciferase was measured for entry. Hashed bars represent chimeric spikes and solid bars represent full-length spikes as shown in panel (**d**). Cells were infected in quadruplicate as technical replicates. For each graph, individual replicates are plotted as points, the mean is shown as a bar and lines indicate standard deviation.

sarbecovirus, SARS-CoV, with RBDs from other sarbecoviruses[25]. The resulting chimeric spike gene was used in viral pseudotype assays to measure entry efficiency in cell culture of a panel of sarbecovirus RBDs[25]. Using this approach (called "SarbecoType"), we previously characterized the cell entry for the majority of all published sarbecovirus RBDs, which led to isolation of new sarbecoviruses, identified understudied cell entry pathways, and helped elucidate the molecular determinants of sarbecovirus cell entry[25–29]. We have also produced chimeric sarbecovirus molecular clones that are capable of replicating with a different receptor tropism when given either a different spike gene or RBD from other sarbecoviruses, further demonstrating the feasibility of exchanging the RBD within this subgenus[30].

In this work, we take a similar approach, called "MerbecoType," with the merbecovirus subgenus of betacoronaviruses. Similar to sarbecoviruses, RBDs of merbecoviruses are classified into four different "clades" based on the presence or absence of indels, which exhibit clade-specific trends in receptor use and cell entry. Surprisingly, at least half of the merbecovirus RBD clades use ACE2 for cell entry, with the entire group of HKU5 viruses exhibiting clear preference for ACE2 from their natural host species, *Pipistrellus abramus* bats. We subsequently validate this result using live virus assays and determine the structure for HKU5 spike trimer and discuss similarities with other bat coronavirus spikes. These findings are important for ongoing efforts to identify looming coronavirus threats and in the development of interventions such as broad-spectrum antivirals and universal coronavirus vaccines.

Results

Mapping the functional receptor binding domain

In order to test a large panel of RBDs from diverse merbecoviruses in viral pseudotype entry assays, MERS-CoV spike expression constructs were engineered to allow for easy replacement of the RBD with an RBD from other merbecoviruses (Fig. 1a–c). MERS-CoV was selected as the recipient spike backbone because of its extensive structural characterization and compatibility with cell-culture based models of merbecovirus entry[1,31–33]. Similar to our prior sarbecovirus study[25], the MERS-CoV spike was codon optimized for human cells, appended with a C-terminal FLAG tag and silent mutations were introduced outside the RBD to produce restriction digest sites for its removal (Fig. 1b). While MERS-CoV uses DPP4 for entry, ACE2 functions as a receptor for some other merbecoviruses including PDF2180 (Fig. 1d)[22]. Thus, the RBD from PDF2180 made an ideal candidate to develop a chimeric MERS-CoV spike and demonstrate successful receptor switching from DPP4 to ACE2 usage, generating a platform to explore different merbecovirus RBD receptor preferences in entry.

To guide construction and expression of chimeric merbecovirus spikes, we utilized available structures. Unfortunately, amino acid motifs that are conserved across all merbecovirus spike sequences are rare, complicating the task of identifying common RBD exchange junctions across the merbecovirus subgenus. However, closer inspection of published spike sequences revealed several highly conserved glycine residues flanking the RBD (MERS-CoV spike positions 372 and 610; Fig. 1a, d, e). These two residues flank the RBD region of

spike used for structures with host receptor molecules[22,34]. While the structures of RBDs have been determined for some merbecoviruses[11,22,34,35], regions flanking the RBD are flexible, making them difficult to structurally resolve in RBD:receptor complexes (Fig. 1a, e, pink shaded region). To maximize chances for successful spike expression, several chimeras between MERS-CoV and PDF2180 were produced: version 1 included the region of PDF2180 spike between the conserved glycines, version 2 consisted of the RBD region within two flexible flanking regions of the HKU4 spike structure, and version 3 was based on the PDF2180-RBD as defined previously (Fig. 1e)[22]. DNA fragments encoding the different RBD fragments were cloned into the MERS-CoV spike backbone and used to generate vesicular stomatitis virus (VSV) single-cycle pseudotypes (Fig. 1c).

VSV-based pseudotypes were evaluated using a cell-based entry assay. While Baby Hamster Kidney cells (BHK cells) are not naturally susceptible to coronavirus entry but can support entry after ectopic receptor expression, BHK cells expressing human ACE2 do not always recapitulate natural viral entry for ACE2-dependent viruses with low affinity for the receptor[29,36]. Therefore, 293 T cells, which exhibit low but not a complete lack of susceptibility to coronavirus entry, were stably transduced to express human ACE2 or DPP4. Infecting these stable cell lines with pseudotypes bearing chimeric spikes revealed that the PDF2180 RBD was able to use human ACE2 for entry, indicating a successful receptor exchange for MERS-CoV spike (Fig. 1d, f; PDF2180 V1). The regions of PDF2180 spike between RBD residues 376-381 and 586-609 were essential for receptor-use exchange, as two other spikes with shorter regions of the PDF2180 RBD were unable to use ACE2 (Fig. 1a, d–f; PDF2180 V2, V3). Addition of exogenous protease (trypsin) during the assay enhanced viral entry, and afforded more sensitive detection of low affinity interactions. Importantly, trypsin-enhanced entry was still receptor dependent (Fig. 1f). Production of a chimeric spike containing an analogous region from the DPP4-dependent HKU4-SM3A virus showed a retention in DPP4 use in MERS-CoV spike[37], further suggesting this region would allow for assessment of diverse receptor preferences (Fig. 1e-f).

Optimizing MERS-CoV spike for pseudotype assays

With an operational RBD-exchange strategy in place, the next goal was to optimize the spike backbone for pseudotype efficiency, which would allow for improved sensitivity to low-level viral entry. After engaging with the host receptor, coronavirus spikes are processed by host-cell proteases to release the spike fusion peptide and mediate membrane fusion[38,39]. While the TMPRSS-family of cell-surface proteases and endosomal cathepsins have been shown to cleave many different coronavirus spikes, including MERS-CoV, SARS-CoV and SARS-CoV-2, furin is another protease that plays an important role in spike biogenesis and cell entry, depending on the availability of an appropriate cleavage site[40–43]. MERS-CoV spike contains furin sites at the S1/S2 and S2′ junctions not found in some other merbecovirus spikes. Because previous studies have shown that removal of the furin site from SARS-CoV-2 spike results in increased pseudotype efficiency[44–46], several versions of chimeric merbecovirus spikes were produced with either one or both furin sites mutated. Additionally, C-terminal truncations in the cytoplasmic tails of MERS-CoV, SARS-CoV and SARS-CoV-2 spikes increase surface expression of spike in transfected cells, resulting in improved pseudotype efficiency[47–49]. Therefore, the protease site mutants were also tested with or without a 16-amino acid truncation in the C-terminal end of MERS-CoV spike (Supplementary Fig. 3a-c). Surprisingly, these modifications to spike had little effects on entry in 293 T cells for MERS-CoV WT, PDF2180 RBD or HKU4/SM3A RBD (Supplementary Fig. 3b-c). While not statistically significant, spikes containing a C-terminal truncation and removal of the S2′ furin site performed slightly better than the other spikes; therefore, this set of modifications was included for further experiments.

Merbecovirus RBD screen reveals a receptor for the HKU5 complex

Genbank has over 2000 entries for “merbecovirus” and “MERS-like” viruses; of these 2000 entries, only about 842 entries contain full-length spike, and of those entries, approximately half are from species other than humans and camels (Fig. 2a). Many coronavirus Genbank listings do not always contain species identifiers in the metadata, which left several MERS-CoV entries remaining even after excluding human and camel viruses. Further eliminating viruses titled as “MERS-CoV” from the list resulted in 65 spike sequences, which encompassed 34 unique RBD sequences (Fig. 2a; Table 1, Supplementary Fig. 1). Some merbecoviruses are likely missing from this list as coronavirus nomenclature has evolved over the years. However, even with these considerations, this curated panel of merbecoviruses spans 18 years of virus discovery (some sequences in this study pre-date the MERS-CoV outbreak), 6 countries and 3 continents (Table 1).

Phylogenetic analysis of the RBD amino acid sequences (as defined between the two glycine residues highlighted in Fig. 1) has revealed several genetically-clustered groups based on characteristic indels and the sequences surrounding them (Fig. 2b, c, Supplementary Fig. 1). The groups were labeled as clades 1 through 4: clade 1 includes MERS-CoV and HKU4 discovered between 2006 and 2012[1,50,51], clade 2 includes HKU5 also discovered in 2006[50], clade 3 incudes the African merbecoviruses, NeoCoV and PDF2180, discovered in 2017[13], and clade 4 includes the contemporary hedgehog merbecoviruses, “ErinCoVs,” discovered in Germany in 2014 and most recently identified in Italy in 2020 (Fig. 2b, c, Table 1)[9,52–54]. RBDs for these merbecoviruses were synthesized and cloned into the optimized MERS-CoV spike backbone plasmid. All chimeric spike plasmids were stably expressed in 293 T cells and used to produce pseudotyped viral-like particles for downstream experiments (Fig. 2d). Concentrated supernatants were positive for the presence of spike by western blot analysis; however, variations observed in spike levels did not correlate with viral entry phenotypes observed in downstream assays (Fig. 2d).

VeroE6 cells were poorly permissive for entry of the pseudotyped merbecovirus RBD panel, with addition of trypsin only mildly improving entry for some of the viruses in a clade-independent manner (Fig. 2e). In contrast, Huh-7.5 cells, a human hepatocellular carcinoma cell line, were more susceptible to clade 1 merbecovirus RBDs (Fig. 2e). Addition of trypsin improved entry for some of the clade 4 viruses for both cell lines (e.g., ErinCoV-1-18 and ErinCov-12-19) (Fig. 2e).

The diverse panel of merbecovirus pseudotypes was tested on 293 T cell lines stably transduced to express known human coronavirus receptors: amino peptidase N (APN), DPP4, or ACE2. In the absence of trypsin, untransduced 293 T cells exhibited poor susceptibility to the entire panel, while APN cells were susceptible to entry with a positive control: human coronavirus 229E, which is known to use APN as an entry receptor (Fig. 2f)[55]. Cells transduced with human DPP4 exhibited clear susceptibility to clade 1 merbecovirus RBDs but not the other clades (Fig. 2f), while cells expressing human ACE2 exhibited low level susceptibility to SARS-CoV-2 spike and clade 3 merbecovirus RBDs (Fig. 2f). Exogenous trypsin moderately increased entry in untransduced 293 T cells for human coronaviruses MERS-CoV and SARS-CoV-2, which uses human DPP4 and human ACE2, respectively, suggesting low levels of the human receptors were present on 293 T cells (Fig. 2f). In the presence of trypsin, clade 1 RBDs entered cells through DPP4, while clades 2, and 3 RBDs entered cells expressing ACE2 (Fig. 2f). APN cells remained susceptible to HCoV-229E entry in the presence of trypsin. While entry signal under tenfold is considered borderline permissive in this assay, and difficult to interpret, there were many viruses that presented low, but consistently detectable levels of ACE2 compatibility (Fig. 2f).

Human cells expressing human ACE2 exhibited low level susceptibility to a wide range of merbeocviruses (Fig. 2). To investigate if

https://doi.org/10.1038/s41467-025-60286-3

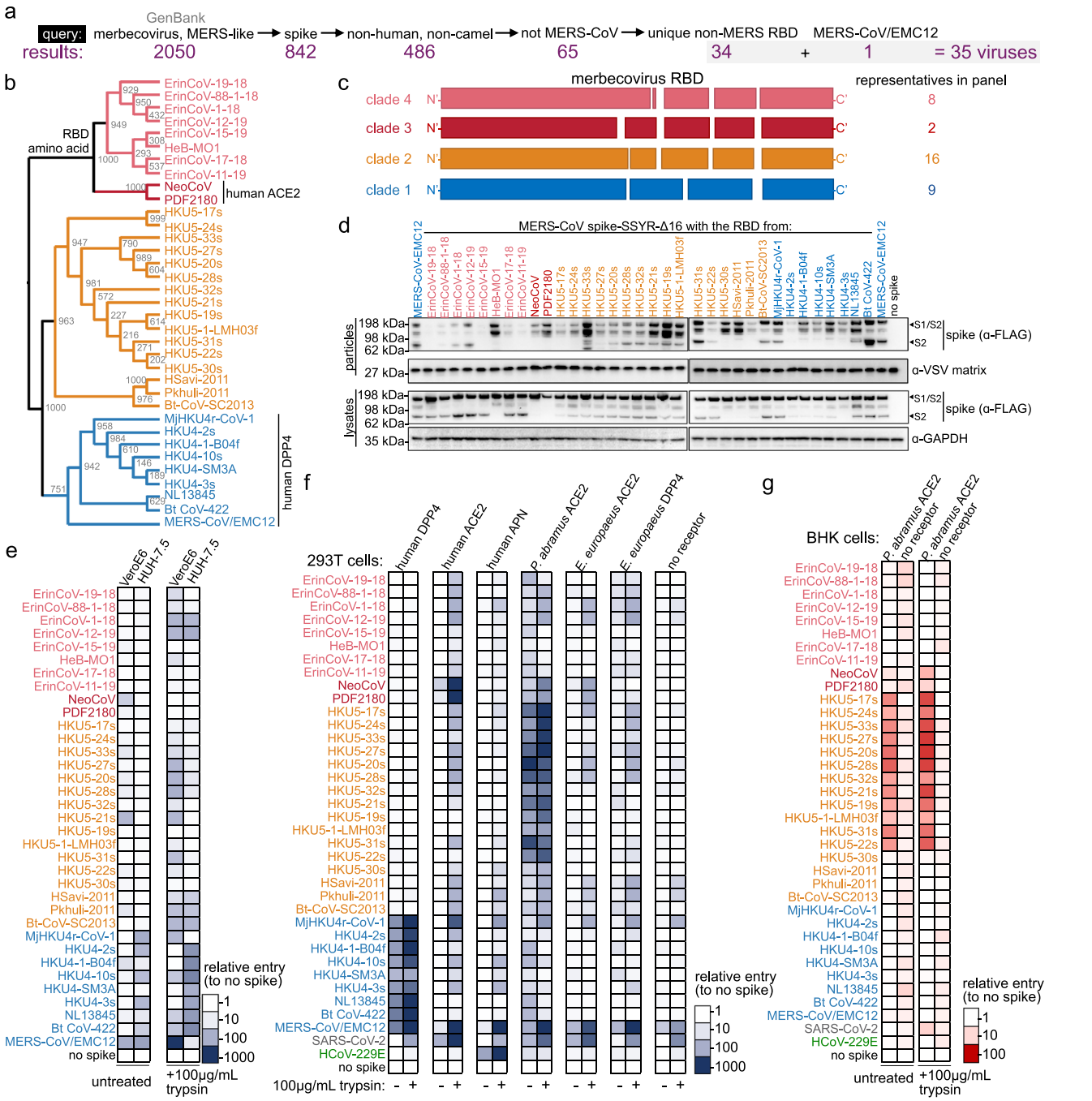

Fig. 2 | Merbecovirus RBDs sort into clades based on sequence and entry phenotype. a Total sequence diversity in merbecoviruses encompasses approximately 34 RBD sequences. **b** Cladogram showing the relationship of RBD amino acid sequences. Known receptors indicated. **c** Schematic overview of RBD clades, indicating the approximate size and location of indels characteristic to each merbecovirus RBD clade. **d** Western blot for FLAG (spike) expression of chimeric spikes. Results shown are representative of multiple biological replicates. **e** VeroE6 cells or Huh-7.5 cells were infected with VSV pseudotype panel bearing indicated chimeric spikes, in quadruplicate as technical replicates. The mean is shown as a bar and lines indicate standard deviation. Luciferase was measured for cell entry. **f** 293 T cells transduced to express human APN, human DPP4 or human ACE2 or transfected with *Erinaceus europaeus* ACE2, *Erinaceus europaeus* DPP4 or *Pipistrellus abramus* ACE2 were infected in the absence or presence of 100 μg/mL trypsin. **g** BHK-21 cells were transiently transfected with empty vector or *Pipistrellus abramus* ACE2, and infected with or without exogenous trypsin. All cells were infected in quadruplicate as technical replicates. Heatmaps represent mean relative entry as compared to pseudotypes without spike.

the merbecovirus RBD panel can use receptor orthologues from their cognate host species, ACE2 and DPP4 were synthesized from European hedgehogs (*Erinaceus europaeus*), the natural host species for the ErinCoVs (Table 1; merbecovirus RBD clade 4), and ACE2 was synthesized from Japanese house bats (*Pipistrellus abramus*): the natural host species for the HKU5 viruses (Table 1; merbecovirus RBD clade 2). DPP4 and ACE2 from European hedgehogs were inefficient as entry receptors and did not mediate entry for any of the merbecovirus clades in the absence of trypsin (Fig. 2f). However, 293 T cells transfected with ACE2 from Japanese house bats were highly permissive for entry by the entire HKU5 cluster of clade 2 merbecovirus RBDs—in the presence or absence of exogenous trypsin (Fig. 2f). As reported in studies by other groups, we observed background entry in 293Ts, which we attributed to low-level expression of known coronavirus

Table 1 | Diverse Merbecovirus panel encompassing global diversity

	Virus	Accession number	Receptor Clade	Host species	Location
1	ErinCoV-19-18	MW246796	4	*Erinaceus europaeus*	Italy
2	ErinCoV-88-1-18	MW246795	4	*Erinaceus europaeus*	Italy
3	ErinCoV-1-18	MW246797	4	*Erinaceus europaeus*	Italy
4	ErinCoV-12-19	MW246800	4	*Erinaceus europaeus*	Italy
5	ErinCoV-15-19	MW246802	4	*Erinaceus europaeus*	Italy
6	HKU31-HeB-MO1	OM451213	4	*Erinaceus amurensis*	China
7	ErinCoV-17-18	MW246798	4	*Erinaceus europaeus*	Italy
8	ErinCoV-11-19	MW246799	4	*Erinaceus europaeus*	Italy
9	NeoCoV	KC869678	3	*Neoromicia capensis*	South Africa
10	PDF2180	KX574227	3	*Pipistrellus hesperidus*	Uganda
11	HKU5-17s	AGP04930	2	*Pipistrellus abramus*	Hong Kong
12	HKU5-24s	AGP04936	2	*Pipistrellus abramus*	Hong Kong
13	HKU5-33s	KC522104	2	*Pipistrellus abramus*	Hong Kong
14	HKU5-27s	AGP04938	2	*Pipistrellus abramus*	Hong Kong
15	HKU5-20s	AGP04933	2	*Pipistrellus abramus*	Hong Kong
16	HKU5-28s	AGP04939	2	*Pipistrellus abramus*	Hong Kong
17	HKU5-32s	AGP04942	2	*Pipistrellus abramus*	Hong Kong
18	HKU5-21s	AGP04934	2	*Pipistrellus abramus*	Hong Kong
19	HKU5-19s	AGP04932	2	*Pipistrellus abramus*	Hong Kong
20	HKU5-1-LMH03f	NC009020	2	*Pipistrellus abramus*	China
21	HKU5-31s	AGP04941	2	*Pipistrellus abramus*	Hong Kong
22	HKU5-22s	AGP04935	2	*Pipistrellus abramus*	Hong Kong
23	HKU5-30s	AGP04940	2	*Pipistrellus abramus*	Hong Kong
24	HSavi-2011	MG596802	2	*Hypsugo savii*	Italy
25	PKhuli-2011	MG596803	2	*Pipistrellus kuhlii*	Italy
26	Bt-CoV-SC2013	KJ473821	2	*Vespertilio superans*	China
27	MjHKU4r-CoV-1	OQ786862	1	*Manis javanica*	China (Smuggled pangolins)
28	HKU4-2s	AGP04916	1	*Tylonycteris pachypus*	Hong Kong
29	HKU4-1-B04f	NC009019	1	*Tylonycteris pachypus*	Hong Kong
30	HKU4-10s	AGP04924	1	*Tylonycteris pachypus*	Hong Kong
31	HKU4/SM3A	MW218395	1	*Tylonycteris pachypus*	Hong Kong
32	HKU4-3s	AGP04917	1	*Tylonycteris pachypus*	Hong Kong
33	NL13845	MG021451	1	*Tylonycteris pachypus*	China
34	Bt-CoV 422	MG021452	1	*Tylonycteris pachypus*	China
35	MERS/EMC12	JX869059	1	*Homo sapiens*	Saudi Arabia

receptors, although we were unable to detect expression of known coronavirus receptors in 293 T cells by westernblot (Supplementary Fig. 4d)[22,56–58]. To account for this background, we normalized entry signal from each pseudotype against its entry in cells without receptor. These normalized results further show the specificity each clade has for its receptor (Supplementary Fig. 3).

To completely eliminate background signal we detected in the entry assays, 293 T cells were exchanged with BHK cells, which are not susceptible to any sarbecovirus or merbecvirus due to significant hamster receptor incompatibilities and poor cell surface expression of known receptors[59,60]. Following transfection with *Pipstrellus abramus* ACE2, BHK cells became highly permissive for HKU5 RBD-mediated entry (Fig. 2g). Notably, all HKU5 sequences derive exclusively from *Pipistrellus abramus* samples (Table 1).

An HKU5 molecular clone utilizes bat ACE2

The previous experiments were performed with human receptor stable cell lines and cells transiently transfected with *Pipistrellus abramus* ACE2. To achieve more consistent entry results with *Pipistrellus abramus* ACE2, a lentiviral vector was produced to generate stable cell lines, following the successful methodologies applied to generate the human receptor cell lines[29,61] (Fig. 3a). Unlike the parental cells, VeroE6 transduced with *Pipistrellus abramus* ACE2 were highly susceptible to the entire HKU5 RBD panel as well as the clade 3 viruses, NeoCoV and PDF2180, but remained poorly susceptible to clade 1, clade 4 and the clade 2 RBDs that were not identified in *Pipistrellus abramus* bats (compare Fig. 2e compared with 3b). To further confirm receptor use for the HKU5 viruses, full-length spike sequences from HKU5-20s and HKU5-21s were synthesized and used to produce viral pseudotypes. For comparison, pseudotypes were also produced with the chimeric MERS-CoV-based spikes used in the previous experiments (Fig. 3c). Full-length HKU5-20s and HKU5-21s spikes were expressed and incorporated into pseudotypes (Fig. 3d). Again, while detection of spike varied across the concentrated pseudotype panel, it did not correspond with the observed entry results (Fig. 3d, e). BHK cells transduced with *Pipistrellus abramus* ACE2 were susceptible to both full-length and chimeric HKU5-20s and −21s spikes but not MERS-CoV, a DPP4-dependent spike (Fig. 3e, f). Altogether, the clear and species-specific entry observed for all HKU5 RBDs and full-length HKU5 spikes exclusively in cells expressing *Pipstrellus abramus* ACE2 strongly support a hypothesis that ACE2 is the natural receptor for these viruses in natural hosts.

https://doi.org/10.1038/s41467-025-60286-3

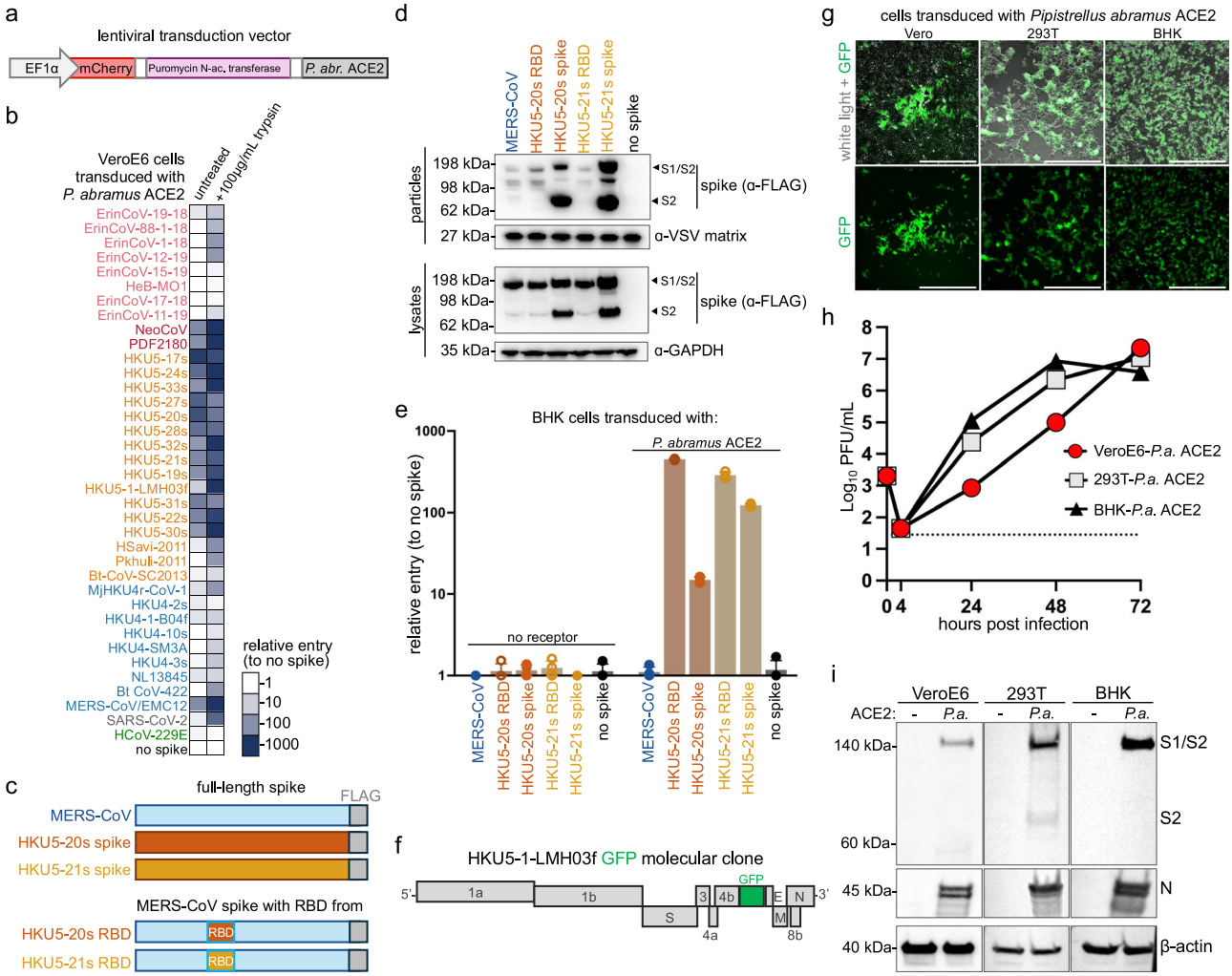

Fig. 3 | *Pipistrellus abramus* ACE2 rescues entry of full-length HKU5 spike in non-susceptible cells. a *Pipistrellus abramus* ACE2 expression cassette used in lentiviral transduction. **b** VeroE6 cells were transduced with *Pipistrellus abramus* ACE2 and infected with chimeric spike pseudotypes in quadruplicate as techincal replicates. The mean is shown as a bar and lines indicate standard deviation. **c** Schematic overview of full length and chimeric spikes. **d** Spike expression in cell lysates and incorporation in pseudotyped particles. **e** BHK-21 cells were transduced to express *Pipistrellus abramus* ACE2 and infected with pseudotypes bearing the indicated spikes. Solid circles represent full length spikes, hollow circles represent chimeric spikes. Cells were infected in quadruplicate as technical replicates. For each graph, individual replicates are plotted as points, the mean is shown as a bar and lines indicate standard deviation. **f** Overview of HKU5 molecular clone with GFP reporter in place of Orf5. **g** Light and fluorescent microscopy of indicated cell lines at 24-h post-infection. Scale bar in lower right corner is 400 μm. Data shown are representative of two biological replicates **h** Growth curve of viral replication as measured by PFU of supernatants at indicated time points. **i** Western blot of infected cells for viral and host proteins at 24-h post-infection.

To confirm if *Pipistrellus abramus* ACE2 could function as a receptor for true virus, we generated a replication competent molecular clone of HKU5 with green fluorescent protein (GFP) cloned in place of Orf5 (Fig. 3f)[24]. Vero cells, 293 T cells or BHK cells stably transduced with *Pipistrellus abramus* all strongly supported efficient viral replication in the absence of trypsin, as evidenced by GFP expression during replication, accumulation of infectious virus as measured by plaque assays, and production of viral spike and nucleocapsid proteins in infected cells (Fig. 3g–i). Detection of distinct spike glycoprotein products at ~180 and 75 kDa strongly support spike proteolytic processing and cleavage due to the presence of a putative furin cleavage site.

To further validate our findings and rule out potential DPP4-mediated entry mechanisms, we generated Huh7.5 cells lacking both ACE2 and DPP4 (Huh7.5 DKO). Functional viral entry assays using authentic live-virus SARS-CoV-2 (ACE2-user) and MERS-CoV (DPP4-user) nanoluciferase (nLuc) reporter viruses confirmed the complete knockout of these receptors, as the Huh7.5 DKO cells were entirely resistant to infection by both viruses. Complementation of *Homo sapiens* ACE2 or DPP4 restored susceptibility to SARS2-CoV-2 and MERS-CoV, respectively. Transient transfection of *Pipistrellus abramus* ACE2 rendered Huh7.5 DKO cells permissive to HKU5-GFP, as demonstrated by accumulation of GFP positive cells and nucleocapsid protein. In contrast, cells transfected with either empty vector control or *Homo sapiens* ACE2 did not support HKU5-GFP replication or entry with other pseudotypes. Western blot analysis confirmed equal expression of both receptors (Supplementary Fig. 4).

HKU5 RBD binds to Pipistrellus abramus ACE2

To assess if HKU5 RBD recognizes *Pipistrellus abramus* ACE2, we performed enzyme-linked immunosorbent assays (ELISAs) using purified recombinant proteins. As controls, we included MERS-CoV RBD, SARS-CoV-2 RBD, and their respective receptors, human DPP4 and human ACE2 (Fig. 4). Increasing amounts of receptors fused to dimeric IgG Fc resulted in dose-dependent binding of MERS-CoV RBD with human DPP4, SARS-CoV-2 RBD with human ACE2, and HKU5-24s RBD with

https://doi.org/10.1038/s41467-025-60286-3

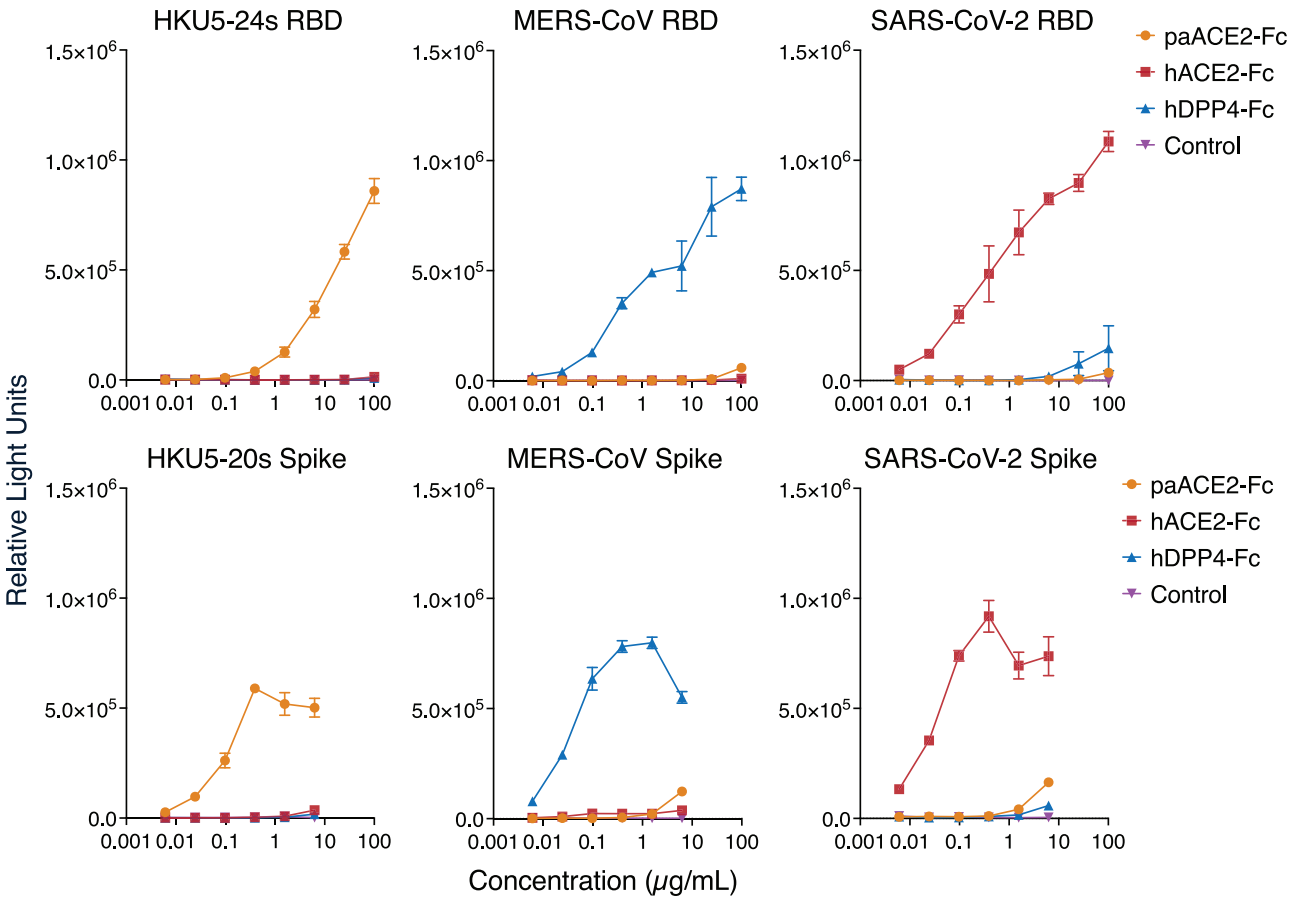

Fig. 4 | Recombinant HKU5 RBD and spike bind to *Pipistrellus abramus* ACE2. Recombinant RBD or spike proteins were immobilized on ELISA plates and incubated with increasing amounts of the indicated receptor-Fc fusion protein or with a BSA-only control. Each data point is the mean of four measurements with bars indicating standard deviations. Binding to *Pipstrellus abramus* ACE2 is indicated in orange lines with circles, human ACE2 is indicated in red lines with squares, and human DPP4 is shown in blue with triangles.

Pipistrellus abramus ACE2. We also observed similar binding profiles with full length spikes (Fig. 4).

Consensus sequences mimic clade-specific entry phenotypes

To further assess clade-specific receptor use, consensus sequences were generated for the RBDs from clades 1, 2 and 4 and used to produce chimeric spikes (Supplementary Fig. 5). PDF2180 was selected as a representative of clade 3 because clade 3 only contains two representative RBD sequences (Fig. 5a). Pseudotypes bearing chimeric consensus RBD spikes generally reflected clade-specific entry phenotypes observed for individual RBDs from previous experiments (Fig. 5b, c), suggesting that features including common amino acid motifs and structural aspects within each RBD clade dictate entry.

HKU5 RBD mutations influence species compatibility

A previous study reported structures of clade 3 merbecovirus RBDs from PDF2180 and NeoCoV bound to ACE2 from *Pipistrellus pipstrellus* bats (Fig. 6a)[22]. To see how the HKU5:ACE2 interface compares with these previous structures, we used AlphaFold 3 to predict the interactions between HKU5 RBDs and *Pipistrellus abramus* ACE2 (Fig. 6b, c, Supplementary Fig. 6)[62]. In the experimentally-determined structure with PDF2180, the interface between the RBD with *Pipistrellus pipistrellus* ACE2 involves multiple interactions with two surface-exposed loops on the RBD (Fig. 6a), which we refer to here as Loop 1 and Loop 2. Interestingly, while both loops were still implicated in the AlphaFold 3 prediction for HKU5 RBDs, their binding site on *Pipistrelllus abramus* ACE2 was different from PDF2180 and *Pipistrellus pipistrellus* ACE2 (Fig. 6a–c, d). Curiously, Loop 2 is highly polymorphic in merbecoviruses, with several HKU5 viruses, but not all, exhibiting a 4 amino acid deletion in this region (Fig. 6b, c; Figure Supplementary Fig. 1b). To assess if an analogous interface is compatible with interactions between HKU5 RBDs and bat ACE2, several sterically bulky or charged amino acid mutations were introduced at two points in the middle of Loops 1 and 2 (Fig. 6). For these mutation experiments, HKU5-20s RBD was selected because it includes both loops and shows strong entry with *Pipistrellus abramus* ACE2, and HKU5-21s RBD was selected because it contains a 4 amino acid deletion in loop 2, while still strongly exhibiting entry using *Pipistrellus abramus* ACE2 (Figs. 2, 3a, Supplementary Fig. 1b). For experimental consistency, BHK cells and 293 T cells were transduced with a lentivector to constitutively express *Pipistrellus abramus* ACE2 and were infected in parallel assays to reduce effects from non-specific variation in the cell line background. Overall, mutations in Loop 2, but not Loop 1, of the HKU5 RBD disrupted entry with *Pipistrellus abramus* ACE2 (Fig. 6f–h). While most of the mutations only reduced spike entry with bat ACE2, mutations in Loop 2 of the HKU5-20s RBD, but not the HKU5-21s RBD, increased entry with cells expressing human ACE2 (Fig. 6h). While this difference was relatively small, the statistically-significant increase in entry was observed across different cell line backgrounds. Importantly, each mutation's effect on viral entry was observed across both the BHK (hamster) and 293T-based (human) cell lines, suggesting the observed

https://doi.org/10.1038/s41467-025-60286-3

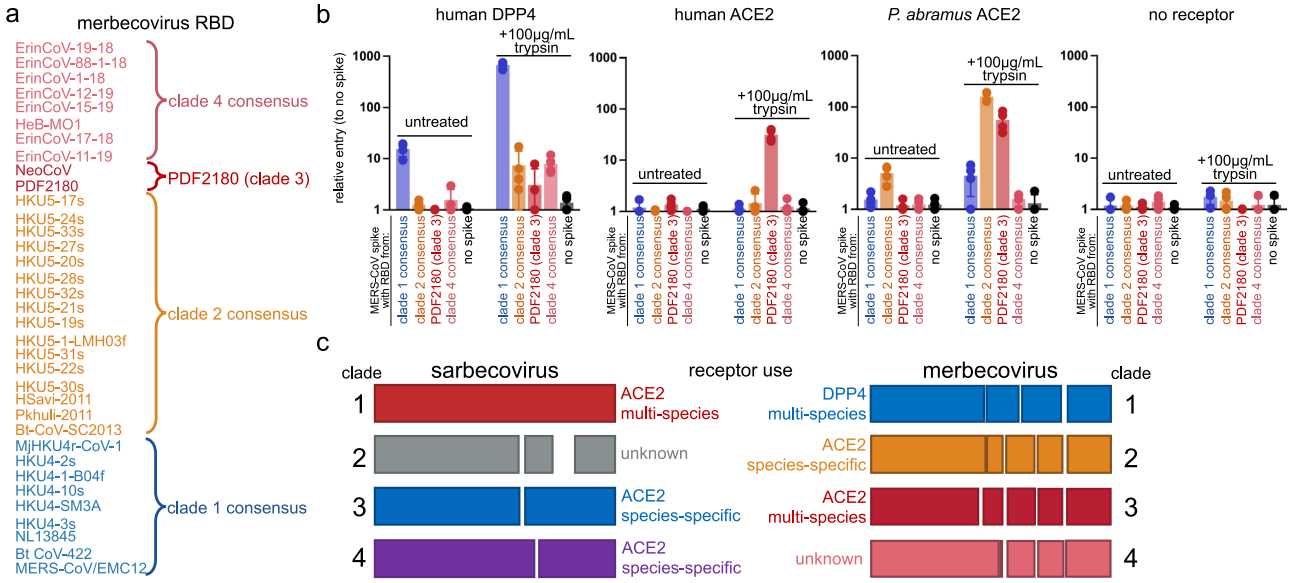

Fig. 5 | Clade consensus RBDs mimic clade-specific entry. a Consensus sequences were generated for clades 1, 2, and 4. **b** 293 T cells transfected with indicated receptors were infected with chimeric spikes bearing clade consensus RBDs, in quadruplicate as technical replicates. The mean is shown as a bar and lines indicate standard deviation. **c** Schematic overview of sarbecovirus and merbecovirus RBD clades, indel patterns and receptor use.

effects derive from the transduced ACE2 rather than other non-specific cell line variation (Fig. 6).

HKU5-20s spike structure reveals all 'down' RBDs

To further assess the interaction between HKU5-20s spike and *Pipistrellus abramus* ACE2 (paACE2), we attempted to solve a single-particle cryo-EM structure of a complex between a 2 P stabilized[63] HKU5-20s trimeric ectodomain and soluble paACE-2 (both monomeric and dimeric paACE2-Fc), preparing grids at room temperature or at 37 ˚C. All grids yielded structures of the HKU5-20s spike trimer only, with no identifiable density for paACE2, suggesting further optimization of the binding conditions is needed for determining a receptor-spike complex structure by cryo-EM. Indeed, prior work assessing merbecovirus spike interactions with *Pipistrellus* ACE2 were only in the context of purified RBD with receptor, not with a spike trimer ectodomain[22].

We processed data from a grid incubated with paACE2-Fc plus HKU5-20s spike trimer ectodomain to derive a 2.8 Å structure of the unbound HKU5 trimer (Supplementary Fig. 7, Supplementary Table 1). The structure revealed the expected S1 and S2 subunit organization as seen in other CoV spike trimers (Fig. 7a–d). Although a distribution of 'up' and 'down' RBDs is usually found for sarbecovirus spike trimers[64,65], we found only 'down' RBDs in the HKU5-20s trimer structure (Fig. 7a, b). To examine the degree of sequence conservation across 10 representative merbecovirus spikes (see "Methods"), we plotted amino acid sequence conservation on surface representations of structures of the HKU5-20s spike protomer and the HKU5-20s RBD (Fig. 7d). We found more conserved regions in S2 and at the base of the RBD (Fig. 7d). The well-resolved densities for the three 'down' RBDs allowed building of an RBD model including coordinates for Loops 1 and 2 (Fig. 7e). These results provide additional structural insights for HKU5-20s spike trimer over an existing HKU4 RBD structure[11], and will be instrumental in future antigen design, e.g., by providing information about which RBD surfaces are accessible in the context of trimeric spike.

Discussion

Compared to sarbecoviruses, which share ≥90% nucleotide sequence identity in their RBDs[25,66], the diversity in merbecovirus RBD sequences is greater, initially complicating the RBD exchange strategy utilized in this study (Figs. 1, 7e; Supplementary Fig. 1). Wide variability between merbecovirus host species (hedgehogs, bats, camels, humans and pangolins) also poses unforeseen challenges when studying cross-species interactions. The chimeric spike approach presented herein aims to eliminate some of the interspecies variability by using the human-compatible MERS-CoV spike as a backbone in experiments performed in human cells and other cells that support MERS-CoV infection. Our studies support the hypothesis that this approach reduces off-target phenotypes relating to cell attachment and protease processing. Addition of exogenous protease bypasses host-cell protease-processing, allowing for assessment of just the RBD interaction in the presence or absence of receptor. As now seen in this study and many others, chimeric coronavirus spikes faithfully re-create entry of both full spikes and wild-type viruses (Figs. 1–3)[25–30,36,61,67].

Merbecovirus RBDs can be classified into four clades based on sequence, characteristic indels, and entry phenotype, but not geographic origin (Figs. 2, 5; Supplementary Fig. 1, Table 1). Results from this study show that clade 1 viruses can use DPP4 from multiple species, clade 2 viruses have species-specific ACE2 preference, and clade 3 can use ACE2 from a wider range of host species. Recently, a merbecovirus found in Russian bats was shown to use ACE2 with a restricted host range, further demonstrating species-specific ACE2 interactions among merbecoviruses[23]. No clear entry was observed with clade 4 viruses and receptors tested here, but nevertheless, some ErinCoVs exhibited minor entry in some human cell lines in the presence of trypsin (Figs. 2e–g, 3b, Supplementary Fig. 4e). Although the data presented here suggest ACE2 and DPP4 are not the receptor for clade 4 merbecoviruses, it is possible these viruses use these receptors in other host species not tested herein, and/or that the approach taken in this study is not suitable for detecting their entry. For example, if a region of ErinCoV spike outside of the RBD boundaries tested here interacts with the host receptor or regulates RBD binding, then the chimeric spike entry assays would miss this interaction. Additionally, while the chimeric spike strategy helps to reduce unforeseen entry barriers, dependence on extra-cellular factors remains possible, but is difficult to anticipate or control[68]. Alternatively, clade 4 merbecovirus RBDs may use a receptor that is neither DPP4 nor ACE2, analogous to sarbecovirus RBD clade 2 viruses, which also can infect human cells through an unidentified route (Figs. 2, 5)[25–28].

https://doi.org/10.1038/s41467-025-60286-3

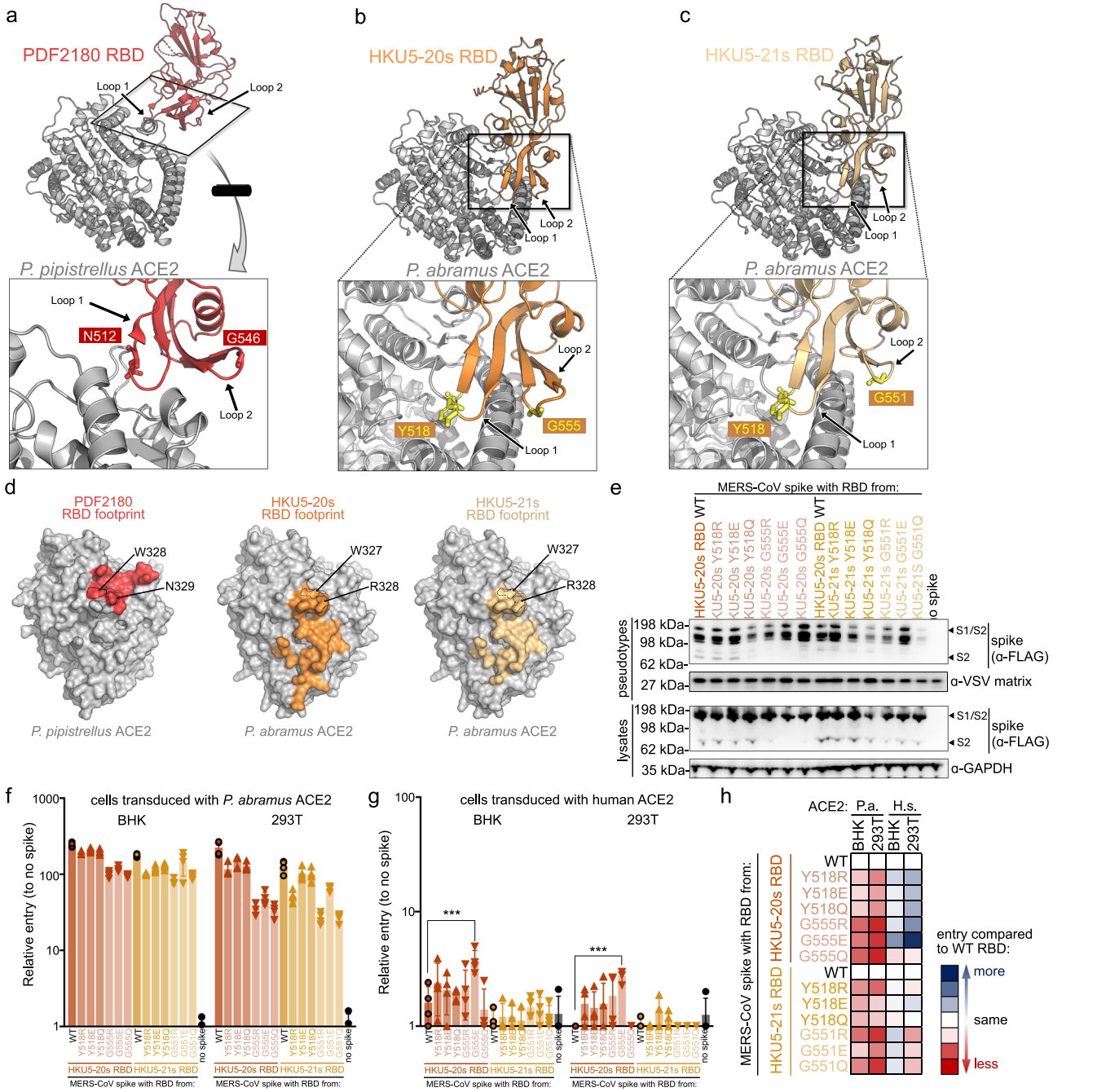

Fig. 6 | Structure-guided mutagenesis at the HKU5:ACE2 interface. a Co-structure for PDF2180 RBD and *Pipistrellus pipistrellus* ACE2 (PDB ID: 7wpz). **b** AlphaFold3 predicted structures for HKU5-20s RBD (residues 390-614) and *Pipistrellus abramus* ACE2 (residues 20-608). **c** AlphaFold3 predicted structure for HKU5-21s RBD (residues 390-609) and *Pipistrellus abramus* ACE2 (residues 20-608). **d** Comparison of viral RBD footprints on species ACE2. **e** Mutant spike expression in cell lysates and incorporation in pseudotyped particles. ACE2 residues common to all three interfaces are highlighted. BHK or 293 T cells transduced with either **f** *Pipistrellus abramus* (P.a.) or **g** human (H.s.) ACE2 were infected with indicated pseudotypes in quadruplicate as technical replicates. Dark circles indicate wildtype sequences, and triangles indicate point mutant sequences. For each graph, four individual entry values are plotted as points, the mean is shown as a bar and lines indicate standard deviation. 2-way ANOVA with Tukey correction for multiple comparisons (***) Indicates *P* value < 0.001. **h** Entry values for mutant RBDs as compared to parental wild-type RBD.

MERS-CoV spike can rapidly adapt to sub-optimal interactions with DPP4 from non-cognate species[61], and the ongoing SARS-CoV-2 pandemic underscores the ability of spike to adapt and correct sub-optimal ACE2 interactions while simultaneously escaping the immune response[69–72]. Other research has shown that clade 3 merbecoviruses gain even broader host ACE2 tropism with a single point mutation in the spike RBD, T510F, significantly increasing tropism for human ACE2[21,22]. Mutagenesis experiments presented here identified a region of HKU5 RBDs that also modifies ACE2 tropism (Fig. 6). Structurally, T510F is on loop 1 of the RBD, while the effective mutations identified in this study are located on the adjacent loop 2 (Fig. 6a–d). Only HKU5-20s, which possesses a larger second loop in its RBD, was able to gain consistent and statistically significant entry using human ACE2, with mutations. By contrast, HKU5-21s, with a shorter surface loop, did not measurably shift in ACE2 tropism (Fig. 6f–h; Supplementary Fig. 1B). These results suggest that deletions within loop 2 of some HKU5

https://doi.org/10.1038/s41467-025-60286-3

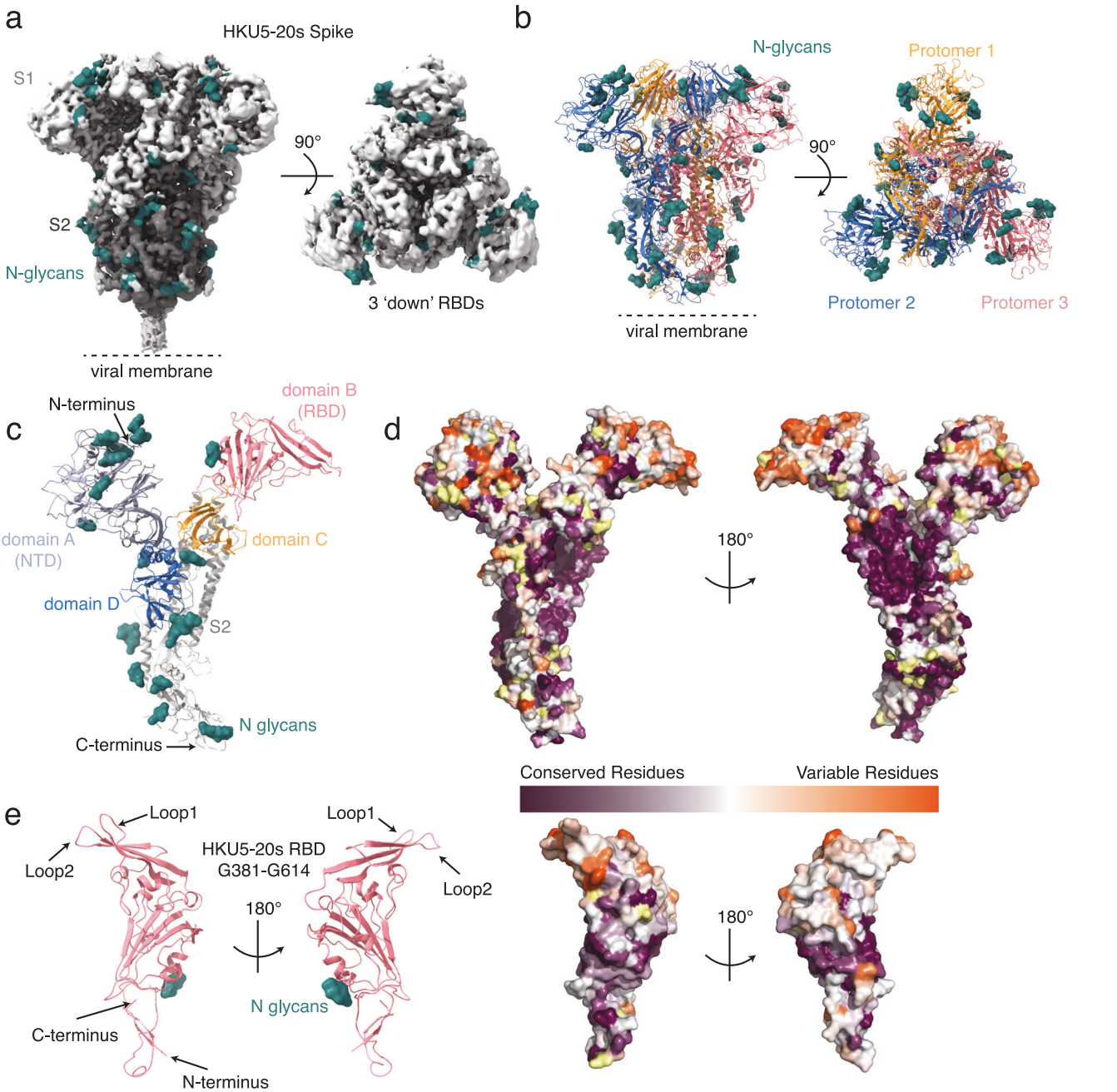

Fig. 7 | Structure of HKU5-20s spike trimer. a EM density of HKU5-20s spike with three 'down' RBDs is shown from the side (left) and top (right). **b** Cartoon diagram of HKU5-20s spike trimer with different colors for each protomers shown from the side (left) and top (right). **c** Cartoon diagram of a spike protomer showing domains A-D. **d** Amino acid sequence conservation of 10 merbecovirus spike sequences calculated by ConSurf Database[102] plotted on a surface representation of an HKU5-20s protomer (top) and HKU5-20s RBD (bottom). Yellow indicates that <10% of the sequences were available for the calculation at that position. **e** Cartoon diagram of the HKU5-20s RBD from two orientations.

viruses may limit their evolutionary adaptability and that a larger second loop, found in spikes such from viruses such as HKU5-20s, may allow for a different ACE2 interactions. These data and AlphaFold3 predictions of the interface between HKU5 and *Pipistrellus abramus* ACE2 suggest HKU5 spike interacts with a different region of ACE2 than has been reported for other merbecoviruses (Fig. 6a–d). Although, closer inspection of PDF2180 and HKU5 RBD interfaces with ACE2 reveals both viruses interact with ACE2 residues 328/329: a region that is also part of the interaction with RBDs from SARS-CoV-1, SARS-CoV-2 and NL63 spikes, implying this region may be a hot spot for viral interactions[19,73,74] (Fig. 6d). Notably, the AlphaFold 3 predicted co-structures presented here are in strong agreement with a cryo-EM co-structure of the HKU5-19s RBD and *Pipistrellus abramus* ACE2 that was reported while we were revising this manuscript (Supplementary Fig. 6)[75]. The surprisingly accurate predictions from AlphaFold 3 suggest this software may be able to predict other novel coronavirus receptor interfaces, and provides additional insights into the possible variation in binding between HKU5 viruses with an enlarged second loop (Fig. 6a–d). Deep mutagenesis scanning and comparative structural studies with both types of HKU5 RBDs are needed to further understand the role of the short and longer loops in the HKU5-RBD interface. An HKU5 virus was detected in several deceased mink in China[76]. Interestingly, the virus found in these animals contained a larger second loop in its RBD, similar to HKU5-20s. Spillover of HKU5

from bats to mink taken together with the low-level human cell compatibility reported here for some of the HKU5 viruses and our mutagenesis results, underscores the need for broadly protective coronavirus vaccines[67,77].

While we were completing this study, a second lineage of HKU5 viruses was identified that exhibited human ACE2 compatibility when trypsin was added to the infection medium[78]. While lineage 2 HKU5 viruses may have broader ACE2 tropism than the lineage 1 viruses tested here, it is notable that many of the HKU5 lineage 1 viruses we tested also exhibited low-level entry in cells expressing human ACE2 when trypsin was included (Fig. 2f) and we have previously shown that our HKU5-1 molecular clone is capable of replicating in human cell lines when supplemented with trypsin[24]. Thus, broader ACE2 compatibility may be an intrinsic and adaptable feature of the HKU5 complex.

Structural studies of other coronavirus spike trimers have revealed a distribution of different conformations with respect to the position of the RBDs[11,65,79]. Coronavirus RBDs on a spike trimer can be in an'up' state, with receptor contact sites being surface-exposed and capable of interacting with host cell receptors, or in the 'down' state, with the receptor contacts buried and inaccessible[11,65,79]. MERS-CoV spike has been observed with one or two RBDs down[80], SARS-CoV spike has been observed with two or three 'down' RBDs[80], and SARS-CoV-2 spike has been observed with zero, one, two or three 'down' RBDs[64,65,81,82]. Analogously, the spike trimer from HCoV-229E, an alphacoronavirus with a tri-partite RBD, has been observed with all 'down' RBDs or some 'up' RBDs[79]. Because the RBD is the primary target of neutralizing antibodies, transitions between'up' and 'down' RBD states is believed to play a role in immune evasion[65,80]. We only observed HKU5-20s spike ectodomains with all 'down' RBDs (Fig. 7). Structures of spike trimers from bat merbecoviruses PDF2180 and NeoCoV, as well as the bat sarbecovirus RsSHC014, have also been observed exclusively with all 'down' RBDs[22,83]. Unlike the human respiratory coronaviruses, all bat coronaviruses have been identified in fecal or other gut-derived samples and are presumed to be gastrointestinal in their hosts[6,12,13]. The low pH in the stomach and protease-rich gastrointestinal tract presents a unique and harsh environment for viruses, which may select for more closed confirmations in coronavirus spikes that have this tissue tropism. How these closed spikes transition to a state that can interact with the receptor is yet to be determined but may involve extracellular factors and/or pH changes[64].

HKU5 viruses were first sequenced in 2006, shown to be DPP4-independent in 2014, and demonstrated to replicate in Vero cells in the presence of exogenous trypsin in 2020[12,24,50]. To date, more than 40 ACE2 orthologues from bats and other species have been tested with HKU5 viruses[6,22,24,84]; however, of all bat ACE2's tested, only ACE2 from *Pipistrellus abramus* mediates entry for these viruses (Figs. 2–5). The RBD from HKU5 viruses shares ~50% amino acid identity with MERS-CoV and clade 1 RBDs, while the RBD from NeoCoV is only ~30-40% identical to MERS-CoV and HKU5 coronaviruses (Supplementary Fig. 1). This low sequence identity between NeoCoV and HKU5 RBDs has confounded efforts to predict the receptor for HKU5 from sequences alone.

A previous study identified ACE2 as the receptor for the clade 3 merbecoviruses such as PDF2180 and closely-related NeoCoV but was unable to identify the receptor for the clade 2 HKU5 viruses[22]. This earlier study assessed the ability of HKU5 to interact with ACE2 from *Pipistrellus pipistrellus* bats and several other Yangochiropteran bats, but not the true host species for HKU5. The clear preference of HKU5 for *Pipistrellus abramus* ACE2, but not other ACE2 species orthologues tested clearly demonstrates a tighter species specificity found within clade 2 RBDs (Figs. 2–3). *Pipistrellus abramus* ACE2 varies from previously tested *P. pipistrellus* and *P. khuli* ACE2s at residues 328 and 329, in close proximity to the interaction site previously reported with NeoCoV/PDF2180 RBDs, potentially explaining why HKU5 RBDs do not bind this orthologue (Fig. 6A-C)[22]. Residue N329 in *Pipistrellus pipistrellus* ACE2 is also N-glycosylated[21], while the corresponding residue in *Pipistrellus abramus* ACE2, R328, is not, which may also explain the striking restriction in receptor use. Similar to the merbecovirus RBD clades, clade 1 sarbecoviruses can use ACE2 from diverse species, while clade 3 sarbecovirus RBDs only interact with ACE2 from their cognate species (Fig. 5c)[36,67].

A clade 1 RBD pangolin merbecovirus has been shown to use human DPP4 and was isolated in Vero81 cells[85]. While Vero cells are frequently used in virus isolation attempts[1,86,87], data from our study suggests that Huh-7.5 cells may be a more suitable cell line for isolating DPP4-dependent merbecoviruses and perhaps even some clade 4 merbecoviruses. The mechanisms underlying why these cells seem to allow more of these viruses to enter is yet to be determined. Furthermore, MERS-CoV grown in Vero cells has been shown to quickly accumulate tissue-culture adaptations in the spike protein driving the need for alternative cell culture models[33].

Merbecoviruses represent yet another type of beta-coronavirus found in wildlife with potential human cell compatibility and a possibility to cause severe disease in humans. Japanese house bats (*Pipistrellus abramus*) are the natural host for HKU5 coronaviruses and are synanthropic, roosting in human dwellings and structures, and therefore pose repeat opportunities for human exposure[50,88]. Although clade 2 merbecovirus RBDs exhibit low human ACE2 compatibility (Figs. 2–6), efforts should still be made to reduce contact with the host animals. The development of replication-competent HKU5 and PDF2180 recombinant viruses will support the development of pan-coronavirus and pan-merbecovirus vaccines and small molecule countermeasures to protect the health of populations globally. The work presented here will serve as a guide to understanding merbecovirus cell entry, subsequent spillover risk and support One Health Preparedness.

Methods

Biosafety

Prior approval for experiments using full-length, recombinantly derived HKU5 was obtained from the Institutional Biosafety Committee of the University of North Carolina at Chapel Hill. All experiments using live HKU5 virus were performed under Biosafety Level 3 conditions with personnel wearing full-body personal protective equipment and HEPA-filtered respiratory protection.

AlphaFold 3 predictions of RBD-receptor interface

To predict the interaction between RBD and receptor, the full amino acid sequence for *Pipistrellus abramus* ACE2 was submitted to AlphaFold 3[62] along with amino acids 381-614 from HKU5-20s or amino acids 381-609 for HKU5-21s. Standard parameters were used for the prediction. Resulting output structures were visualized in PyMol (Schrodinger Software; version 3.1.4). For structural depictions in Fig. 6, the HKU5 RBDs in the AlphaFold 3 predictions were trimmed to amino acid 390 for better comparison with previously published structural data.

Cells and viruses

293T (ATCC CRL-3216), VeroE6 (ATCC CRL-1586), Huh-7.5 (Cellosaurus CVCL_7927) and BHK-21 (ATCC CCL-10) cells were maintained in DMEM (Gibco) supplemented with 10% FBS (GE HyClone), penicillin-streptomycin (Gibco), and L-glutamine (Gibco) and maintained at 37 °C and 5% CO_2. Cells stably expressing coronavirus receptors were generated as previously described and maintained under selection with either 1 μg/mL puromycin (Fisher; BHK and 293 T) or 5 μg/mL puromycin (VeroE6)[29]. Briefly, cells were infected with lentiviral transduction vectors expressing viral receptors and puromycin N-acetyl transferase and subsequently placed under puromycin selection approximately one week post-transduction. Cells were maintained under puromycin selection during the entire study. All cell

lines were species-confirmed with cytochrome sequencing and verified mycoplasma negative with MycoSniff PCR Kit (MP Bio). No commonly misidentified cells were employed for this study. The molecular clone derived HKU5-GFP was generated as previously described[24]. Briefly, genomic cDNA sequences were ligated, in vitro transcribed, and electroporated into BHK cells. Stocks of recombinant HKU5-GFP were then propagated in Vero cells stably expressing *Pipistrellus abramus* ACE2. Recombinant SARS-CoV-2 and MERS-CoV nanoluciferase (nLuc) reporter viruses were propagated VeroE6/ACE2/TMPRSS2 and Vero81 cells, respectively. All live viruses were grown at 37 °C and 5.0% CO_2. For multistep growth curve analysis, cells were infected at an MOI of 0.01. Samples of infected cell culture supernatant were collected at 0, 4, 24, 48, and 72 h.p.i. and stored at −80 °C for titration via plaque assay. For fluorescent microscopy and western blot experiments, cells were infected with HKU5-GFP at an MOI of 1.0. At 24 h.p.i., GFP-fluorescence was monitored using an inverted optical microscope (Olympus, IX73), and lysates were harvested for western blot analysis as described below.

Cryo-EM sample preparation

paACE2-spike trimer and paACE2-Fc–spike trimer complexes were prepared by incubating purified paACE2 or paACE2-Fc with HKU5-20s trimer at a molar ratio of 3:1 (paACE2 or pACE2-Fc:spike trimer) at 37 °C for 30 min to a final concentration of ~2 mg/mL. Cryo-EM grids were prepared using a Mark IV Vitrobot (ThermoFisher) operating at 37 °C and 100% humidity. Sample (3 µL) was applied to a 300 mesh Quantifoil R1.2/1.3 grids (Electron Microscopy Sciences) that had been freshly glow discharged with a PELCO easiGLOW (Ted Pella) for 1 min at 20 mA. Grids were blotted for 3 seconds with Whatman No.1 filter paper and grids were vitrified in liquid ethane. Tweezers were pre-heated to 37 °C before picking up grids.

Cryo-EM data collection and processing

A single-particle cryo-EM dataset for HKU5-20s spike 2 P with paACE2-Fc was collected using SerialEM automated data collection software[89] on a 200 keV Talos Arctica cryo-electron microscope (Thermo Fisher Scientific) equipped with a K3 camera (Gatan) (Supplementary Table 1). Movies were recorded with 40 frames, a defocus range of −1 to −3 µm, and a total dosage of 60 e-/Å^2 using a 3x3 beam image shift pattern in the super-resolution mode with a pixel size of 0.4345 Å. Movies were motion corrected with patch motion correction using a binning factor of 2, and CTF parameters were estimated using Patch CTF in cryoSPARC v4.5.3[90]. Particle picking was done with blob picker in cryoSPARC using a particle diameter of 100–200 Å, and movies and picked particles were inspected before extraction. Particles were extracted and classified using 2D classification in cryoSPARC. Particles from selected 2D classes were used for template picker with a particle diameter of 150 Å. Picked particles were inspected before extraction and 2D classification. Particles from selected classes were used for ab initio reconstruction with 4 volumes and heterogeneous refinement in cryoSPARC. Subsequent homogeneous and non-uniform refinements were carried out, and the final reconstruction was obtained from a non-uniform refinement conducted with C3 symmetry in cryoSPARC.

Structure figures were made using ChimeraX[91]. For plotting sequence conservation onto protein structure surfaces, sequence alignments of 10 representative merbecovirus spikes were performed using Geneious Prime (https://www.geneious.com). Conservation scores for analogous residues (HKU5-20s residues 24-1231 for spike protomer and residues 381-614 for RBD) were calculated and mapped onto the HKU5-20s protomer or RBD by using ConSurf[92]. The following 10 merbecovirus spike sequences were used in the sequence alignment:

- GenBank AFS88936 (MERS-CoV-EMC/2012)
- GenBank AGP04933 (HKU5-20s)
- GenBank AGP04934 (HKU5-21s)
- GenBank AGY29650 (NeoCoV)
- GenBank AHY61337 (BtVs-BetaCoV/SC2013)
- GenBank ARJ34226 (PDF2180)
- GenBank AUM60014 (Bat-CoV/H.savii)
- GenBank AUM60024 (Bat-CoV/P.khulii)
- GenBank QRN68031 (ErinCoV-19/2018)
- GenBank USL83011 (MOW15-22/2015)

MERS-CoV/EMC12 was selected because of high sequence identity with HKU5 spikes[12]; NeoCoV, PDF2180 and MoW-15-22 spikes were selected because they have been shown to use ACE2[21,22,23]; BatCoV/PKhuli, H.Savii, and SC2013 were selected as other clade 2 RBDs to compare with HKU5 RBD (Supplementary Fig. 1), and the clade 4 RBD from ErinCoV-19-18 was selected because of low sequence identity with other merbecovirus RBD clades (Supplementary Fig. 1).

ELISAs

ELISAs were performed using a Tecan Evo liquid handling robot as described[93]. 384-well Nunc MaxiSorp ELISA plates (Millipore Sigma) were coated with 2.5 µg/mL of purified RBD or spike in 0.1 M $NaHCO_3$ pH 9.8 and incubated at 4 °C overnight. For blocking, plates were aspirated and 3% bovine serum albumin (BSA) was added. Plates were incubated at room temperature for an hour. Blocking solution was washed with Tris-buffered saline with 0.1% Tween 20 (TBST). 100 µg/mL or 6.25 µg/mL of a receptor-Fc fusion protein was serially diluted by fourfold using TBST with 3% BSA and added to the plates. After a 2-h incubation at room temperature, plates were washed with TBST and incubated with a secondary HRP-conjugated goat anti-human IgG Fc (SouthernBiotech) at a 1:100,000 dilution for an hour at room temperature. Plates were washed with TBST and developed using SuperSignal ELISA Femto Maximum Sensitivity Substrate (Thermo Fisher Scientific) and relative light units (RLU) were at 425 nm. Mean signals calculated for each quadruplicate measurement were plotted with standard deviations using Graphpad Prism v10.4.0.

Generation of Huh7.5 CRISPR KO and trans-complementation cells

Huh7.5 receptor double knock out cells (ACE2/DPP4 DKO cells) were generated using CRISPR/Cas9 gene editing. A single guide RNA targeting exon 6 of ACE2 (5′- CGGCCAGTTGATTGAAGATGTGG-3′) and exon 9 of DPP4 (5′- GCAGTACCCAAAGACTGTACGGG′-3) were synthesized (IDT DNA) and cloned into the pLentiCRISPv2 vector Addgene, #52961 harboring puromycin or blasticidin resistance genes, respectively. The gRNA constructs were then transfected using Lipofectamine 3000 (Invitrogen, #L3000008) with packaging plasmids into HEK293T cells, and lentiviruses were harvested 72 h later. Huh7.5 cells were subsequently co-transduced and selected using puromycin (2.5 ug/ml) and blasticidin (10 ±ug/ml) for 2 weeks prior to single cell sorting into 96-well plates using a FACS ARIA II flow cytometer. Monoclonal cell populations were then used for subsequent experiments. For experiments with SARS-CoV-2-nLuc and MERS-CoV-nLuc, *Homo sapiens* ACE2 and DPP4 were cloned into the sleeping beauty transposon plasmid, pSB-RFP-Neo (Addgene, #60522) and transfected along with transposase, pCMV(CAT)T7-SB100 (Addgene, #34879), into Huh7.5 DKO cells. Cells were stably selected with neomycin (Fisher; 20 ug/ml) for 2 weeks. For experiments with HKU5-GFP, *Pipistrellus abramus* ACE2 was transiently transfected into Huh7.5 DKO cells 24 h prior to infection in 6 well plates.

Phylogenetic analysis

The amino acid sequences for spike receptor binding domains aligned using Clustal multiple sequence alignment software and default parameters. A maximum likelihood phylogenetic tree was produced with PhyML v. 3.0[94]. The 'WAG' matrix +G model of amino acid substitution was selected by the Smart Model

Selection method with 1000 bootstrap replicates[95]. A tree was then visualized as a cladogram with FigTree v1.4.4 (https://github.com/rambaut/figtree). Clade consensus sequences were generated with the aid of Geneious (Dotmatics, Inc.).

Pipistrellus abramus ACE2 cell lines

Pipistrellus abramus ACE2 was sub-cloned from expression plasmid into a lentiviral expression vector with PCR and used to produce lentiviral particles in 293 T cells[61,96]. Supernatants were filtered, aliquoted and frozen at −80 °C. BHK cells, 293 T cells and VeroE6 cells were transduced with a lentiviral expression vector as previously described[29,61]. Cells were maintained for 3 passages under selective pressure before use in experiments.

Plasmids

MERS-CoV/EMC12 spike (accession number JX869059) was codon optimized, appended with C-terminal FLAG tag, and silent mutations were introduced near spike amino acids 341 and 617 to generate AflII and NotI restriction digest sites. RBDs were codon optimized for human cells and synthesized (IDT DNA)[25]. Lyophilized RBD fragments were resuspended in water and used in downstream Infusion based cloning (Takara Bio) reactions to assemble full-length chimeric spike proteins. *Erinaceus europaeus* ACE2, transcript variant 1 (genbank XM_060183012.1), *Pipistrellus abramus* ACE2 (genbank GQ262782.1) and *Erinaceus europaeus* DPP4 (genbank XM_060177812.1) were codon optimized, split in half and synthesized for Infusion based DNA assembly. Splitting genes into multiple parts reduces synthesis time, costs and overall synthesized product complexity. A complete list of accession numbers for the spike panel can be found in Table 1.

Protein Expression for cryo-EM

A trimeric HKU5-20s trimeric ectodomain (residues 24-1301 of the GenBank sequence AGP04933) with 2 P stabilizing mutations[63], a mutated furin cleavage site between S1 and S2, a C-terminal TEV site, foldon trimerization motif, 8xHis tag, and AviTag was expressed as described[97]. A gene encoding a 8xHis-tagged soluble paACE2 (*Pipistrellus abramus* ACE2) construct (residues 20-613 of the Genbank sequence ACT66266) or a soluble paACE2-Fc (residues 20-613 of Genbank sequence ACT66266 fused to human IgG1 Fc) were expressed and purified as described for human ACE2 and human ACE2-Fc[98] by nickel-NTA (ACE2) or protein A (paACE2-Fc) chromatography followed by size-exclusion chromatography using a Superdex 200 column (Cytiva) as described[99]. Peak fractions were identified by SDS-PAGE, and those containing spike trimer, paACE2, or paACE2-Fc were pooled, concentrated, and stored at 4 ˚C until use.

Pseudotype production

Pseudotypes were generated as previously described[25,28,29]. 293 T cells were seeded in poly-lysine treated 6-well plates and transfected with spike plasmids 24-h later using polyethyleneimine (Poly Sciences). 24-h post transfection, cells were infected with VSV-g-pseudotype VSV particles at a multiplicity of infection of two in serum-free media for one hour, washed three times to remove seed particles and left in serum free media. 48-h post infection, pseudotypes were collected, clarified by centrifugation, aliquoted and stored at −80 °C.

Pseudotype entry assay

Entry assays were performed using standard approaches[26,27]. For human ACE2, APN, and DPP4 experiments, 293 T cells stably transduced with potential coronavirus receptors were seeded in black 96-well plates and subsequently infected 24 h later with equal volumes of viral pseudotypes. For experiments where receptors were transfected, cells were transfected with receptor plasmids and infected 24 h later. Infections were performed on ice to prevent unintended, premature trypsin activity. Pseudotypes were combined with either HBSS or HBSS containing trypsin (not TPCK-treated) to achieve a final concentration of 100 µg/mL trypsin. Cells were washed once with cold PBS, centrifuged with pseudotypes at 4 °C, 1200 × *g* for 1 h and incubated at 37 °C overnight. Luciferase was measured using Bright-Glo reagent (Promega) approximately 18 h post-infection. Relative entry was calculated by dividing raw luciferase values for each spike by the signal for no-spike pseudotypes. To compensate for plate reader background error, plates were measured 4 times, analyzed individually and then averaged across all four measurements. Relative entry values for all four replicates were averaged and plotted as heatmaps using Microsoft Excel.

Live virus entry assay

Authentic live virus entry assays were performed in Huh7.5 DKO cells trans-complemented with coronavirus receptors seeded in black 96-well plates and subsequently infected 24 h later with SARS-CoV-2-nLuc or MERS-CoV-nLuc. Luciferase was measured using NanoGlo Luciferase Assay System in a GloMax plate reader (Promega) 24 h post infection.

Statistics and reproducibility

Each figure with cell entry data that is representative of four technical replicates. Four technical replicates were chosen to maximize statistical relevance, while still allowing for scalable experiments. During this study, experiments were performed with different batches of pseudotypes and cells and at different times. Therefore, the results shown are representative of the observed biological replicates. Statistical significance for mutation comparisons in Fig. 5 were determined by 2-way ANOVA with Tukey correction for multiple comparisons (GraphPad Prism v.9.5.1).

Structure prediction and docking

MERS-CoV spike RBD bound to DPP4 (PDB ID: 4L72)[35], the MERS-CoV spike trimer (PDB ID: 5×59)[80], and the co-structure of NeoCoV-RBD with P. pipistrellus ACE2 (PDB ID: 7WPZ)[22], were visualized in PyMol (version 2.4.0). Structures for HKU5-20s and HKU5-21s RBDs were predicted with SwissModel using PDB IDs 8SAK and 5XGR, respectively[34,100]. *Pipistrellus abramus* ACE2 was modeled with similar methods using PDB ID 7C8J as a guide[101].

Western blot

As described previously[25], 293 T cells transfected with spike plasmids were lysed in 1% SDS lysis buffer and stored at −80 °C until use. Lysates were clarified, boiled, reduced and equivalent volumes of lysate were separated on 10% Bis-Tris gels in MOPS buffer (Invitrogen NuPage)[25]. Pseudotypes were concentrated over iodixanol (Opti-Prep; Sigma) gradients as previously described[25,28,29]. Membranes were probed with FLAG:HRP conjugated monoclonal antibody (ThermoFisher, 1:10,000), GAPDH monoclonal (ThermoFisher, 1:10,000), MERS-CoV N (Sino Biological; catalog number: 40068-RP02; 1:2000), MERS-CoV S2 (Invitrogen; catalog number: 66008-1-Ig; 1:5000) and reprobed with a secondary goat-anti-mouse:HRP poloyclonal mix (ThermoFisher, 1:5000), goat-anti-rabbit-HRP (Cell Signaling Technology; catalog number: 7074S; 1:5000), or goat anti-mouse-HRP (Cell Signaling Technology; catalog number: 7076S; 1:5000). Expression of human orthologues of known coronavirus receptors was measured in Huh-7.5 ACE2/DPP4 double KO cells with the following antibodies: ACE2 (Cell Signaling Technology - 4355S, 1:2000), DPP4 (Cell Signaling Technology - 67138S, 1:2000), APN (Cell Signaling Technology - 1372S, 1:2000) beta-actin (Proteintech - 66009-1-Ig, 1:2000).

Reporting summary

Further information on research design is available in the Nature Portfolio Reporting Summary linked to this article.

Data availability

Accession numbers for all spike sequences used in this study can be found in Table 1. Atomic models and cryo-EM maps generated from cryo-EM studies of the HKU5-20s spike have been deposited at the Protein Data Bank (PDB) and Electron Microscopy Data Bank (EMDB) under accession codes PDB 9D4T and EMBD-46569, respectively. All plotted numerical values from the figures as well as uncropped westernblot images in this study are provided in the supplementary information/source data file. Source data are provided with this paper.

References

1. Zaki, A. M., van Boheemen, S., Bestebroer, T. M., Osterhaus, A. D. & Fouchier, R. A. Isolation of a novel coronavirus from a man with pneumonia in Saudi Arabia. *N. Engl. J. Med.* **367**, 1814–1820 (2012).
2. Dudas, G., Carvalho, L. M., Rambaut, A. & Bedford, T. MERS-CoV spillover at the camel-human interface. *Elife* **7**, https://doi.org/10.7554/eLife.31257 (2018).
3. Dudas, G. & Rambaut, A. MERS-CoV recombination: implications about the reservoir and potential for adaptation. *Virus Evol.* **2**, vev023 (2016).
4. Moreno, A. et al. Detection and full genome characterization of two beta CoV viruses related to Middle East respiratory syndrome from bats in Italy. *Virol. J.* **14**, 239 (2017).
5. Luo, C. M. et al. Discovery of Novel Bat Coronaviruses in South China that use the same receptor as middle east respiratory syndrome coronavirus. *J. Virol* **92**, https://doi.org/10.1128/JVI.00116-18 (2018).
6. Lau, S. K. et al. Genetic characterization of Betacoronavirus lineage C viruses in bats reveals marked sequence divergence in the spike protein of pipistrellus bat coronavirus HKU5 in Japanese pipistrelle: Implications for the origin of the novel Middle East respiratory syndrome coronavirus. *J. Virol.* **87**, 8638–8650 (2013).
7. Ithete, N. L. et al. Close relative of human Middle East respiratory syndrome coronavirus in bat, South Africa. *Emerg. Infect. Dis.* **19**, 1697–1699 (2013).
8. He, W. T. et al. Virome characterization of game animals in China reveals a spectrum of emerging pathogens. *Cell* **185**, 1117–1129 e1118 (2022).
9. De Sabato, L. et al. Can Coronaviruses Steal Genes from the Host as Evidenced in Western European Hedgehogs by EriCoV Genetic Characterization? *Viruses* **12**, https://doi.org/10.3390/v12121471 (2020).
10. Chen, J. et al. A bat MERS-like coronavirus circulates in pangolins and utilizes human DPP4 and host proteases for cell entry. *Cell* **186**, 850–863 e816 (2023).
11. Wang, Q. et al. Bat origins of MERS-CoV supported by bat coronavirus HKU4 usage of human receptor CD26. *Cell Host Microbe* **16**, 328–337 (2014).
12. Yang, Y. et al. Receptor usage and cell entry of bat coronavirus HKU4 provide insight into bat-to-human transmission of MERS coronavirus. *Proc. Natl. Acad. Sci. USA* **111**, 12516–12521 (2014).
13. Anthony, S. J. et al. Further Evidence for Bats as the Evolutionary Source of Middle East Respiratory Syndrome Coronavirus. *MBio* **8**, https://doi.org/10.1128/mBio.00373-17 (2017).
14. Raj, V. S. et al. Dipeptidyl peptidase 4 is a functional receptor for the emerging human coronavirus-EMC. *Nature* **495**, 251–254 (2013).
15. Park, J. E. et al. Proteolytic processing of Middle East respiratory syndrome coronavirus spikes expands virus tropism. *Proc. Natl. Acad. Sci. USA* **113**, 12262–12267 (2016).
16. Li, W. et al. Identification of sialic acid-binding function for the Middle East respiratory syndrome coronavirus spike glycoprotein. *Proc. Natl. Acad. Sci. USA* **114**, E8508–E8517 (2017).
17. Li, F. Receptor recognition and cross-species infections of SARS coronavirus. *Antivir. Res* **100**, 246–254 (2013).
18. Li, F. Structure, function, and evolution of coronavirus spike proteins. *Annu Rev. Virol.* **3**, 237–261 (2016).
19. Li, F., Li, W., Farzan, M. & Harrison, S. C. Structure of SARS coronavirus spike receptor-binding domain complexed with receptor. *Science* **309**, 1864–1868 (2005).
20. Li, W. et al. Receptor and viral determinants of SARS-coronavirus adaptation to human ACE2. *EMBO J.* **24**, 1634–1643 (2005).
21. Ma, C. et al. Broad host tropism of ACE2-using MERS-related coronaviruses and determinants restricting viral recognition. *Cell Discov.* **9**, 57 (2023).
22. Xiong, Q. et al. Close relatives of MERS-CoV in bats use ACE2 as their functional receptors. *Nature* **612**, 748–757 (2022).
23. Ma, C.-B. et al. Multiple independent acquisitions of ACE2 usage in MERS-related coronaviruses. *biorxiv* (2024).
24. Menachery, V. D. et al. Trypsin treatment unlocks barrier for zoonotic bat coronavirus infection. *J. Virol* **94**, https://doi.org/10.1128/JVI.01774-19 (2020).
25. Letko, M., Marzi, A. & Munster, V. Functional assessment of cell entry and receptor usage for SARS-CoV-2 and other lineage B betacoronaviruses. *Nat. Microbiol.*, https://doi.org/10.1038/s41564-020-0688-y (2020).
26. Guo, H. et al. Isolation of ACE2-dependent and -independent sarbecoviruses from Chinese horseshoe bats. *J. Virol.* **97**, e0039523 (2023).
27. Guo, H. et al. ACE2-independent bat sarbecovirus entry and replication in human and bat cells. *mBio* **13**, e0256622 (2022).
28. Khaledian, E. et al. Sequence determinants of human-cell entry identified in ACE2-independent bat sarbecoviruses: A combined laboratory and computational network science approach. *EBioMedicine* **79**, 103990 (2022).
29. Seifert, S. N. et al. An ACE2-dependent Sarbecovirus in Russian bats is resistant to SARS-CoV-2 vaccines. *PLoS Pathog.* **18**, e1010828 (2022).
30. Becker, M. M. et al. Synthetic recombinant bat SARS-like coronavirus is infectious in cultured cells and in mice. *Proc. Natl. Acad. Sci. USA* **105**, 19944–19949 (2008).
31. Almazan, F. et al. Engineering a replication-competent, propagation-defective Middle East respiratory syndrome coronavirus as a vaccine candidate. *mBio* **4**, e00650–00613 (2013).
32. Mou, H. et al. The receptor binding domain of the new Middle East respiratory syndrome coronavirus maps to a 231-residue region in the spike protein that efficiently elicits neutralizing antibodies. *J. Virol.* **87**, 9379–9383 (2013).
33. Scobey, T. et al. Reverse genetics with a full-length infectious cDNA of the Middle East respiratory syndrome coronavirus. *Proc. Natl. Acad. Sci. USA* **110**, 16157–16162 (2013).
34. Han, X. et al. Structure of the S1 subunit C-terminal domain from bat-derived coronavirus HKU5 spike protein. *Virology* **507**, 101–109 (2017).
35. Wang, N. et al. Structure of MERS-CoV spike receptor-binding domain complexed with human receptor DPP4. *Cell Res* **23**, 986–993 (2013).
36. Roelle, S. M., Shukla, N., Pham, A. T., Bruchez, A. M. & Matreyek, K. A. Expanded ACE2 dependencies of diverse SARS-like coronavirus receptor binding domains. *PLoS Biol.* **20**, e3001738 (2022).
37. Lau, S. K. P. et al. Isolation of MERS-related coronavirus from lesser bamboo bats that uses DPP4 and infects human-DPP4-transgenic mice. *Nat. Commun.* **12**, 216 (2021).
38. Millet, J. K. & Whittaker, G. R. Host cell entry of Middle East respiratory syndrome coronavirus after two-step, furin-mediated activation of the spike protein. *Proc. Natl. Acad. Sci. USA* **111**, 15214–15219 (2014).

39. Millet, J. K. & Whittaker, G. R. Host cell proteases: Critical determinants of coronavirus tropism and pathogenesis. *Virus Res.* **202**, 120–134 (2015).
40. Glowacka, I. et al. Evidence that TMPRSS2 activates the severe acute respiratory syndrome coronavirus spike protein for membrane fusion and reduces viral control by the humoral immune response. *J. Virol.* **85**, 4122–4134 (2011).
41. Hoffmann, M. et al. SARS-CoV-2 Cell Entry Depends on ACE2 and TMPRSS2 and Is Blocked by a Clinically Proven Protease Inhibitor. *Cell* **181**, 271–280 e278 (2020).
42. Shirato, K., Kawase, M. & Matsuyama, S. Middle East respiratory syndrome coronavirus infection mediated by the transmembrane serine protease TMPRSS2. *J. Virol.* **87**, 12552–12561 (2013).
43. Shirato, K., Kawase, M. & Matsuyama, S. Wild-type human coronaviruses prefer cell-surface TMPRSS2 to endosomal cathepsins for cell entry. *Virology* **517**, 9–15 (2018).
44. Wang, Z. et al. Loss of furin site enhances SARS-CoV-2 spike protein pseudovirus infection. *Gene* **856**, 147144 (2023).
45. Hoffmann, M., Kleine-Weber, H. & Pohlmann, S. A Multibasic Cleavage Site in the Spike Protein of SARS-CoV-2 Is Essential for Infection of Human Lung Cells. *Mol. Cell* **78**, 779–784 e775 (2020).
46. Bestle, D. et al. TMPRSS2 and furin are both essential for proteolytic activation of SARS-CoV-2 in human airway cells. *Life Sci. Alliance* **3**, https://doi.org/10.26508/lsa.202000786 (2020).
47. Fukuma, A. et al. Inability of rat DPP4 to allow MERS-CoV infection revealed by using a VSV pseudotype bearing truncated MERS-CoV spike protein. *Arch. Virol.* **160**, 2293–2300 (2015).
48. Petit, C. M. et al. Genetic analysis of the SARS-coronavirus spike glycoprotein functional domains involved in cell-surface expression and cell-to-cell fusion. *Virology* **341**, 215–230 (2005).
49. Chen, H. Y. et al. Cytoplasmic tail truncation of SARS-CoV-2 spike protein enhances titer of pseudotyped vectors but masks the effect of the D614G mutation. *J. Virol.* **95**, e0096621 (2021).
50. Woo, P. C. et al. Molecular diversity of coronaviruses in bats. *Virology* **351**, 180–187 (2006).
51. van Boheemen, S. et al. Genomic characterization of a newly discovered coronavirus associated with acute respiratory distress syndrome in humans. *mBio* **3**, https://doi.org/10.1128/mBio.00473-12 (2012).
52. Lau, S. K. P. et al. Identification of a Novel Betacoronavirus (Merbecovirus) in Amur Hedgehogs from China. *Viruses* **11**, https://doi.org/10.3390/v11110980 (2019).
53. Monchatre-Leroy, E. et al. Identification of Alpha and Beta Coronavirus in Wildlife Species in France: Bats, Rodents, Rabbits, and Hedgehogs. *Viruses* **9**, https://doi.org/10.3390/v9120364 (2017).
54. Corman, V. M. et al. Characterization of a novel betacoronavirus related to middle East respiratory syndrome coronavirus in European hedgehogs. *J. Virol.* **88**, 717–724 (2014).
55. Yeager, C. L. et al. Human aminopeptidase N is a receptor for human coronavirus 229E. *Nature* **357**, 420–422 (1992).
56. Eiring, P. et al. Coronaviruses use ACE2 monomers as entry-receptors. *Angew. Chem. Int Ed. Engl.* **62**, e202300821 (2023).
57. Ou, X. et al. Characterization of spike glycoprotein of SARS-CoV-2 on virus entry and its immune cross-reactivity with SARS-CoV. *Nat. Commun.* **11**, 1620 (2020).
58. Si, J. Y. et al. Sarbecovirus RBD indels and specific residues dictating multi-species ACE2 adaptiveness. *Nat. Commun.* **15**, 8869 (2024).
59. Peck, K. M. et al. Glycosylation of mouse DPP4 plays a role in inhibiting Middle East respiratory syndrome coronavirus infection. *J. Virol.* **89**, 4696–4699 (2015).
60. van Doremalen, N. et al. Host species restriction of Middle East respiratory syndrome coronavirus through its receptor, dipeptidyl peptidase 4. *J. Virol.* **88**, 9220–9232 (2014).
61. Letko, M. et al. Adaptive evolution of MERS-CoV to species variation in DPP4. *Cell Rep.* **24**, 1730–1737 (2018).
62. Jumper, J. et al. Highly accurate protein structure prediction with AlphaFold. *Nature* **596**, 583–589 (2021).
63. Pallesen, J. et al. Immunogenicity and structures of a rationally designed prefusion MERS-CoV spike antigen. *Proc. Natl. Acad. Sci. USA* **114**, E7348–E7357 (2017).
64. Zhou, T. et al. Cryo-EM structures of SARS-CoV-2 spike without and with ACE2 reveal a pH-dependent switch to mediate endosomal positioning of receptor-binding domains. *Cell Host Microbe* **28**, 867–879 e865 (2020).
65. Costello, S. M. et al. The SARS-CoV-2 spike reversibly samples an open-trimer conformation exposing novel epitopes. *Nat. Struct. Mol. Biol.* **29**, 229–238 (2022).
66. Boni, M. F. et al. Evolutionary origins of the SARS-CoV-2 sarbecovirus lineage responsible for the COVID-19 pandemic. *Nat. Microbiol* **5**, 1408–1417 (2020).
67. Starr, T. N. et al. ACE2 binding is an ancestral and evolvable trait of sarbecoviruses. *Nature*, https://doi.org/10.1038/s41586-022-04464-z (2022).
68. Earnest, J. T. et al. The tetraspanin CD9 facilitates MERS-coronavirus entry by scaffolding host cell receptors and proteases. *PLoS Pathog.* **13**, e1006546 (2017).
69. Zhang, S. et al. Bat and pangolin coronavirus spike glycoprotein structures provide insights into SARS-CoV-2 evolution. *Nat. Commun.* **12**, 1607 (2021).
70. Wrobel, A. G. et al. SARS-CoV-2 and bat RaTG13 spike glycoprotein structures inform on virus evolution and furin-cleavage effects. *Nat. Struct. Mol. Biol.* **27**, 763–767 (2020).
71. Wrobel, A. G. et al. Evolution of the SARS-CoV-2 spike protein in the human host. *Nat. Commun.* **13**, 1178 (2022).
72. Calvaresi, V. et al. Structural dynamics in the evolution of SARS-CoV-2 spike glycoprotein. *Nat. Commun.* **14**, 1421 (2023).
73. Lan, J. et al. Structure of the SARS-CoV-2 spike receptor-binding domain bound to the ACE2 receptor. *Nature* **581**, 215–220 (2020).
74. Wu, K., Li, W., Peng, G. & Li, F. Crystal structure of NL63 respiratory coronavirus receptor-binding domain complexed with its human receptor. *Proc. Natl. Acad. Sci. USA* **106**, 19970–19974 (2009).
75. Park, Y. J. et al. Molecular basis of convergent evolution of ACE2 receptor utilization among HKU5 coronaviruses. *Cell*, https://doi.org/10.1016/j.cell.2024.12.032 (2025).
76. Zhao, J. et al. Farmed fur animals harbour viruses with zoonotic spillover potential. *Nature* **634**, 228–233 (2024).
77. Starr, T. N. et al. Deep mutational scanning of SARS-CoV-2 receptor binding domain reveals constraints on folding and ACE2 binding. *Cell* **182**, 1295–1310 e1220 (2020).
78. Chen, J. et al. Bat-infecting merbecovirus HKU5-CoV lineage 2 can use human ACE2 as a cell entry receptor. *Cell*, https://doi.org/10.1016/j.cell.2025.01.042 (2025).
79. Song, X. et al. Cryo-EM analysis of the HCoV-229E spike glycoprotein reveals dynamic prefusion conformational changes. *Nat. Commun.* **12**, 141 (2021).
80. Yuan, Y. et al. Cryo-EM structures of MERS-CoV and SARS-CoV spike glycoproteins reveal the dynamic receptor binding domains. *Nat. Commun.* **8**, 15092 (2017).
81. Toelzer, C. et al. Free fatty acid binding pocket in the locked structure of SARS-CoV-2 spike protein. *Science* **370**, 725–730 (2020).
82. Yan, R. et al. Structural basis for the different states of the spike protein of SARS-CoV-2 in complex with ACE2. *Cell Res* **31**, 717–719 (2021).
83. Tse, A. L. et al. Distinct pathway for evolution of enhanced receptor binding and cell entry in SARS-like bat coronaviruses. *bioRxiv*, https://doi.org/10.1101/2024.06.24.600393 (2024).

84. Lau, S. K. P. et al. Replication of MERS and SARS coronaviruses in bat cells offers insights to their ancestral origins. *Emerg. Microbes Infect.* **7**, 209 (2018).
85. Xia, L. Y. et al. Isolation and characterization of a pangolin-borne HKU4-related coronavirus that potentially infects human-DPP4-transgenic mice. *Nat. Commun.* **15**, 1048 (2024).
86. Ogando, N. S. et al. SARS-coronavirus-2 replication in Vero E6 cells: replication kinetics, rapid adaptation and cytopathology. *J. Gen. Virol.* **101**, 925–940 (2020).
87. Kiesslich, S. & Kamen, A. A. Vero cell upstream bioprocess development for the production of viral vectors and vaccines. *Biotechnol. Adv.* **44**, 107608 (2020).
88. Wang, W. et al. Airport noise disturbs foraging behavior of Japanese pipistrelle bats. *Ecol. Evol.* **12**, e8976 (2022).
89. Mastronarde, D. N. Automated electron microscope tomography using robust prediction of specimen movements. *J. Struct. Biol.* **152**, 36–51 (2005).
90. Punjani, A., Rubinstein, J. L., Fleet, D. J. & Brubaker, M. A. cryoSPARC: algorithms for rapid unsupervised cryo-EM structure determination. *Nat. Methods* **14**, 290–296 (2017).
91. Pettersen, E. F. et al. UCSF ChimeraX: Structure visualization for researchers, educators, and developers. *Protein Sci.* **30**, 70–82 (2021).
92. Ashkenazy, H. et al. ConSurf 2016: an improved methodology to estimate and visualize evolutionary conservation in macromolecules. *Nucleic Acids Res* **44**, W344–W350 (2016).
93. Escolano, A. et al. Sequential immunization of macaques elicits heterologous neutralizing antibodies targeting the V3-glycan patch of HIV-1 Env. *Sci. Transl. Med* **13**, eabk1533 (2021).
94. Guindon, S. et al. New algorithms and methods to estimate maximum-likelihood phylogenies: assessing the performance of PhyML 3.0. *Syst. Biol.* **59**, 307–321 (2010).
95. Lefort, V., Longueville, J. E. & Gascuel, O. SMS: Smart model selection in PhyML. *Mol. Biol. Evol.* **34**, 2422–2424 (2017).
96. Letko, M., Booiman, T., Kootstra, N., Simon, V. & Ooms, M. Identification of the HIV-1 Vif and human APOBEC3G protein interface. *Cell Rep.* **13**, 1789–1799 (2015).
97. Fan, C. et al. Neutralizing monoclonal antibodies elicited by mosaic RBD nanoparticles bind conserved sarbecovirus epitopes. *Immunity* **55**, 2419–2435 e2410 (2022).
98. Chan, K. K. et al. Engineering human ACE2 to optimize binding to the spike protein of SARS coronavirus 2. *Science* **369**, 1261–1265 (2020).
99. Barnes, C. O. et al. SARS-CoV-2 neutralizing antibody structures inform therapeutic strategies. *Nature* **588**, 682–687 (2020).
100. Tse, L. V. et al. A MERS-CoV antibody neutralizes a pre-emerging group 2c bat coronavirus. *Sci. Transl. Med.* **15**, eadg5567 (2023).
101. Liu, K. et al. Cross-species recognition of SARS-CoV-2 to bat ACE2. *Proc. Natl. Acad. Sci. USA* **118**, https://doi.org/10.1073/pnas.2020216118 (2021).
102. Landau, M. et al. ConSurf 2005: The projection of evolutionary conservation scores of residues on protein structures. *Nucleic Acids Res.* **33**, W299–W302 (2005).

Acknowledgements

We would like to thank Dr. Stephanie Seifert, Dr. Alex Cohen, Dr. Tyler Starr and Dr. Thomas Gallagher for providing valuable insights and comments on the work and manuscript. We also thank Andy DeLaitsch for his thoughtful and careful review of the manuscript. Research reported in this publication was supported by the National Institute of Allergy and Infectious Diseases of the National Institutes of Health (NIAID/NIH) under Award Numbers R01AI179720 to M.L., R01 AI167966 and CEIRS Contract 75N93021C00014 to R.S.B., P01AI100148 to P.J.B. and T32AI007025 to V.J. The content is solely the responsibility of the author and does not necessarily represent the official views of the National Institutes of Health.

Author contributions

N.J.C., Z.W., C.F., V.J., A.A., A.S., B.L.Y., and M.L. performed experiments, analysis. N.J.C., Z.W., V.J. and M.L. generated figures. P.J.B., R.B. and M.L. provided supervision and funding. M.L. developed the project concept and coordinated collaboration. All authors contributed to the manuscript and approved the final version of the text and figures.

Competing interests

RSB is a member of advisory boards for VaxArt, Takeda and Invivyd, and has collaborative projects with Gilead, J&J, and Hillevax, focused on unrelated projects. The remaining authors compare no competing interests.

Additional information

Supplementary information The online version contains supplementary material available at https://doi.org/10.1038/s41467-025-60286-3.

Correspondence and requests for materials should be addressed to Michael Letko.

Peer review information *Nature Communications* thanks Kenneth Matreyek who co-reviewed with Brent Shassberger, and the other, anonymous, reviewer(s) for their contribution to the peer review of this work. A peer review file is available.